Physical and biological functioning in Proterozoic rivers: evidence from the archetypal pre-vegetation alluvium of the Torridon Group, NW Scotland

WILLIAM J. MCMAHON*† ‡ and NEIL S. DAVIES†

† *Department of Earth Sciences, University of Cambridge, Downing Street, Cambridge CB2 3EQ, United Kingdom*
‡ *Present Address: Utrecht University, Faculty of Geosciences, Princetonlaan 8a, 3584, CB, Utrecht, Netherlands*
* *Corresponding author: w.j.mcmahon@uu.nl*

ABSTRACT

In modern rivers, vegetation affects hydrological, geomorphological and sedimentological functioning, so extant fluvial systems can provide only partial analogues for those rivers that operated before the evolution of land plants. However, pre-vegetation rivers were the norm for the first 90% of Earth history and so a better understanding of their sedimentary product can provide insights into both the fundamental underlying mechanisms of river behaviour and the ways in which fluvial processes operated on ancient Earth. In addition to a short review of the history of research into pre-vegetation alluvium, this paper presents a fieldwork-based case study of the later Proterozoic Torridon Group, which contains some of the most extensive and easily accessible exposures of pre-vegetation alluvium worldwide. Three alluvial architectural deposits have been recognized: 1) channel-bedform deposits (c. 80%); 2) barform deposits (c. 20%); and 3) out-of-channel deposits (<<1%). Channel- bedform deposits have erosional bases and most frequently stack vertically to form thick multistorey channel-bedform sequences. The preferential preservation of these deposits, which record the deepest parts of river channels, suggests that channel migration had a dominant control on preservation in the Torridon Group. Less frequently, channel-bedform deposits pass upwards into a genetically-related barform deposit. Barform preservation in these instances is interpreted to be due to channel avulsion, which protected the barforms from reworking. Channel-bar thickness, measured from the basal erosional surface of a channel-bedform deposit to

the top of its associated barform deposit, indicates minimum water depths of 1.7 to 8.0 m. Downstream-accreting barform deposits are most frequent, but lateral and upstream modes of accretion are also well represented. Dominant southeastward palaeoflow directions imply that the Torridonian rivers were sourced from the Grenvillian Mountain Belt. The preserved architectural deposits and narrow dispersal of palaeocurrent data is explained by interpreting the Torridon Group as the alluvium of dominantly low-sinuosity rivers, with signatures recording autogenic fluvial adjustments. In the few rare instances where out-of-channel deposits are preserved, they contain fossil evidence for microbial mats, which prove that not all Proterozoic river systems were wholly abiotic. The overall characteristics of the Torridon alluvium, in terms of its ubiquitous highly-tabular beds of sand-grade or coarser material, make it an archetypal example of pre-vegetation alluvium as known globally.

1. FLUVIAL PROCESSES AND DEPOSITS IN THE ABSENCE OF LAND PLANTS: INTRODUCTION

Vegetation can play a fundamental role in the operation of modern fluvial systems and the character of their landforms and sedimentary deposits (e.g., Corenblit et al., 2007, 2009; Wohl, 2013; Gurnell, 2014; Horton et al., 2017; Kleinhans et al., 2018). One way in which this fact is emphasized is that Earth's sedimentary-stratigraphic record contains alluvial strata deposited prior to the evolution of land plants (473 – 471 Ma [Rubinstein et al., 2010]), and this 'pre-vegetation' alluvium is sedimentologically-distinct from younger equivalents (Cotter, 1978; Davies and Gibling, 2010a; Long, 2011; Davies et al., 2017; McMahon and Davies, 2018). A better understanding of the properties of pre-vegetation alluvium, and the processes which led to its deposition, is required in order to reveal details of the abiotic skeleton that underpins the rivers that traverse the Earth's continents at the present day.

This paper focuses on explaining the sedimentary architecture of one of the best known examples of pre-vegetation alluvium, the Torridon Group of the northwest Scottish Highlands. This unit has been

51 the subject of geological investigation for over two hundred years (e.g., MacCulloch, 1819; Sedgwick
52 and Murchison, 1829; Peach et al., 1907; Stewart, 2002) but no previous studies have described the
53 sedimentary architecture across all areas of the unit's 200 x 30 km outcrop belt. In this study we
54 rectify this omission and aim to promote the Torridon Group as a reference point from which to
55 examine how Earth's riverine landscapes were transformed following the Palaeozoic evolution of
56 land plants. This paper first gives a concise history of previous research into pre-vegetation alluvium
57 globally (Section 2) in order to contextualize the observations and interpretations of Torridon
58 alluvium which follow (Sections 3-5). We then discuss the utility of the Torridon Group as an
59 archetype for global pre-vegetation alluvium (Section 6), before analyzing biological functioning in
60 pre-vegetation rivers using the physical evidence for microbial life in the succession (Section 7). Our
61 study emphasizes that Proterozoic rivers were not necessarily abiotic systems. However, the
62 commonality of their alluvial characteristics arose from the infrequency of physical controls that, in
63 modern rivers, can be heavily influenced by the physiological and mechanical attributes of riparian
64 flora.

65 **2. PRE-VEGETATION ALLUVIUM: HISTORY OF RESEARCH**

66 *2.1. Early discussions of pre-vegetation alluvium (1930-1979)*

67 It has long been recognized that the evolution of land plants had a significant impact on Earth surface
68 processes. Kaiser (1931) discussed how the hydrological cycle would have been different,
69 emphasizing the problem of modern analogue as there are no rivers devoid of plant life on the surface
70 of Earth today. This observation remains valid: there are no accurately reported instances of modern
71 streams that lack any form of flora at some point along their length. Vogt (1941) specifically
72 considered the effects that a lack of vegetation had on ancient river systems. In a study of Devonian
73 alluvial strata in Spitsbergen, he ascribed an observed upwards increase in weathered mineral grain
74 proportion to a Middle Devonian increase in vegetation cover and substrate protection. Few other

workers around this time explicitly picked up on the value of vegetation in sedimentological interpretations, but Russell (1956) did note that ancient Earth surface processes could only be understood with reference to the character of contemporaneous vegetation, and suggested splitting geological history into: 1) pre-vegetation time; 2) time during colonization of alluvial areas by primitive vegetation; 3) time during colonization by flowering plants; and 4) time following the appearance of grasses.

The rise of the facies model paradigm in the 1960's and 70's (e.g., Allen, 1964; Walker, 1976), saw an increasing attempt to categorise the sedimentary facies of pre-vegetation alluvium, under the recognition that its deposition differed from that in extant fluvial systems. Schumm (1968) used data from modern, sparsely vegetated alluvial catchments to show that pre-vegetation rivers would have operated under far greater rates of denudation and surface runoff. He suggested that large floods would have resulted in the deposition of sheets of (predominantly coarse) sediment, decreasing the likelihood of the development of meandering channel patterns. Cotter (1978) expanded on these ideas, using sedimentary geological data from Ordovician-Carboniferous alluvial formations in the Appalachian Basin, which revealed that clearly channelized architectural deposits were highly uncommon within pre-vegetation alluvium at outcrop scale. Emphasizing the difference, he introduced the term 'sheet-braided' to refer to a distinct rock-architecture property (although he explicitly stated that this was not a description of original fluvial geomorphology: see Table 2). At the same time, Long (1978) recognised the scarcity of fine-grained clastic material within Proterozoic alluvium, which he explained by: 1) a dominance of bedload deposition; 2) high vulnerability of overbank deposits to subsequent reworking; 3) the removal of fines from fluvial systems as wash load; and 4) lower rates of mud production (lower chemical weathering) in the absence of land plants. He also noted the difficulties in determining a marine or fluvial origin for thick sandstone-dominated successions lacking palaeontological indicators. He emphasized that any previous

interpretations of meandering rivers from pre-vegetation alluvium had been based solely on unreliable criteria (e.g., fining-up profiles and palaeocurrent variation).

2.2. The rise of pre-vegetation facies models (1980-2009)

Following on from the work of Schumm (1968), Cotter (1978) and Long (1978), many studies into pre-vegetation alluvium were undertaken during the last two decades of the twentieth century. In a speculative paper, Fuller (1985) suggested that pre-vegetation rivers could have had width:depth ratios in excess of 1000:1, due to the absence of bank-stabilizing vegetation. Other researchers also noted the size discrepancy between ancient and modern rivers, suggesting that pre-vegetation braidplains could have been enormous due to the frequent switching of unstable channels (e.g., Rainbird, 1992; MacNaughton et al., 1997). In terms of planform, a consensus of interpretations implied that the majority of pre-vegetation rivers were braided from source to sink, and terminated in braid-deltas at the shoreline (McPherson et al., 1987; Els, 1998; Sønderholm and Tirsgaard, 1998; Hadlari, 2006) regardless of gradient. High run-off rates were also commonly inferred, leading to the conclusion that pre-vegetation rivers were more sensitive to climate change than their modern counterparts; explaining rapid stratigraphic transitions between perennial and ephemeral characteristics within their alluvium (Tirsgaard and Øxnevad, 1998). The influence of land plants on aeolian processes within the alluvial realm was also subject to scrutiny, leading to the conclusion that, in pre-vegetation settings the absence of plant related baffling and binding meant greater wind-reworking of non-marine deposits (Dalrymple et al., 1985; Fuller, 1985; Eriksson and Simpson, 1998; Tirsgaard and Øxnevad, 1998). The knock-on effect that an absence of land plants had on marine environments was also considered, as common thick, offshore siliciclastic successions were attributed to greater rates of fluvial and aeolian sediment supply (Dott and Byers, 1981; Dalrymple et al., 1985; Lindsey and Gaylord, 1992; Dott, 2003).

2.3. Recent studies of pre-vegetation alluvium (2010-2019)

While much work had begun to focus on pre-vegetation alluvium, Davies and Gibling (2010a,b, 2013) updated Cotter's (1978) study into alluvium from the interval of geological history when vegetation evolved and expanded. Through an extensive analysis of reported Cambrian to Carboniferous alluvial formations, they confirmed that alluvium post-dating Ordovician land plant evolution has a far greater abundance of mudrock, and architectural elements such as laterally-accreting inclined heterolithic stratification, most frequently interpreted as the sedimentary expression of point bar migration within a sinuous channel. In contrast, pre-vegetation alluvium was almost uniformly comprised of 'sheet-braided' sandstones, *sensu* Cotter (1978) (Table 2). Davies and Gibling (2010a,b) noted how this had the effect that the proportion of previous interpretations of 'meandering' versus 'braided' river facies increased in stratigraphic synchrony with the fossil record of land plants. They explicitly emphasized that "the presence of Precambrian and extraterrestrial meandering systems indicates that vegetation is not essential for meandering" (Davies and Gibling, 2010b, p. 51), but that the shift in ratio of braided:meandering interpretations implied that observable sedimentary facies differed in strata deposited before and after the evolution of land plants. One lithological characteristic - the increased occurrence of mudrock in alluvium - was further quantified by Davies et al. (2017) and McMahon and Davies (2018a), who showed that alluvium deposited after plant evolution saw an upsurge in the proportion of preserved mudrock: on average, 1.4 orders of magnitude greater than the proportion contained within pre-vegetation alluvium.

Long (2011, 2019) updated his 1978 review of pre-vegetation alluvium using architectural element analysis (Miall, 1985). He considered sandy braided systems, dominated by sandy-bedforms and downstream-accretion elements, to be the most abundant fluvial style; while recognising that ephemeral channelized, and unconfined deposits filled with upper flow regime elements, were also particularly common. Long (2011) suggested that sandy meandering systems could be identified within pre-vegetation alluvium by measuring the directional relationships between foresets and their underlying bounding surfaces. The commonness of sinuous pre-vegetation channel planforms

148 was subsequently considered in multiple studies (e.g., de Almeida et al., 2016; Santos and Owen,
149 2016; Hartley et al., 2018; Ielpi et al., 2018; McMahon and Davies, 2018c), with the general consensus
150 arising that, while much evidence of genuine pre-vegetation sinuosity may have gone unrecognized
151 (or be unrecognizable), sinuous channel planforms were almost certainly less common on Earth in
152 the absence of biological stabilizing agents, prior to the evolution of land plants. Since the widespread
153 preservation of mud is an important element for more easily classifying fluvial style, we add the
154 caveat that it may be more difficult to diagnose fluvial style in pre-vegetation successions.

155 While some confusion has arisen because the neologism 'sheet-braided rivers' has recently appeared
156 in published literature (de Almeida et al., 2016; Ielpi and Rainbird, 2016), deviating from Cotter's
157 (1978) description of the 'sheet-braided' *architectural style*, the near-ubiquitous architecture has
158 now been demonstrated to likely be the result of many different fluvial channel-patterns (Santos et
159 al., 2014; McMahon and Davies, 2018b). It has also been shown that, whilst alluvial successions may
160 appear monotonous at outcrop scale, exceptional exposure and satellite imagery can sometimes
161 reveal larger scale architectural complexity (Ielpi et al., 2017), and the recognition of barform
162 deposits with similar dimensions to those of modern, deep rivers is helping dispel notions that pre-
163 vegetation river channels were *ubiquitously* broad and shallow (e.g., Ielpi and Rainbird, 2015; Lowe
164 and Arnott, 2016; Went, 2017; Ghinassi and Ielpi, 2018).

165 The extent to which Earth's early vegetation bioengineered Palaeozoic rivers is still discussed from
166 different palaeobotanical (e.g., Edwards et al., 2015), geological (e.g., Davies et al., 2017),
167 geomorphological (e.g., Santos et al., 2019) and modelling (e.g., Kleinhans et al., 2018; Ganti et al.,
168 2019) standpoints, which sometimes, inevitably, lead to apparently contradictory conclusions. To
169 help these move towards a consensus, more detailed sedimentological descriptions of ancient
170 alluvium are needed in order to accurately compare and contrast alluvium deposited by rivers before
171 and after the evolution of land plants.

3. THE TORRIDONIAN SANDSTONES

This study presents a fieldwork-based case study from the later Proterozoic 'Torridonian Sandstones' of the NW Scottish Highlands, which is one of the most extensive and easily accessible exposures of pre-vegetation alluvial strata known globally. The >10 km thick succession of Proterozoic siliciclastic strata is divided into, from oldest to youngest, the Stoer, Sleat and Torridon groups (Fig. 1). The youngest of these is the focus of this study.

The Torridon Group itself is c. 6 km thick and detrital zircon populations (Krabbendam et al., 2017) suggest that it was deposited between approximately 1070 Ma and 990 Ma ago (Mesoproterozoic (Stenian) to Neoproterozoic (Tonian)). The group is divided into four formations; which are, from oldest to youngest:

1) The Diabaig Formation, which infills up to 400-metre-deep palaeotopographic depressions in the Lewisian Gneiss basement (Rodd and Stewart, 1992; McMahon and Davies, 2018c). Alluvial fan breccias and sandstones transition vertically and laterally into lacustrine siltstones. The sedimentological characteristics of the Diabaig Formation are considered in Section 7.1, with additional details available in Callow et al. (2011) and McMahon and Davies (2018c).

2) The Applecross Formation (up to 3000 metres thick), which forms the bulk of the Torridon Group's internal stratigraphy. It near ubiquitously consists of amalgamated, tabular coarse- to pebbly-sandstone deposits and to date has been widely interpreted to have been deposited by low-sinuosity, braided rivers (e.g., Nicholson, 1993; Ielpi and Ghinassi, 2015; Ghinassi and Ielpi, 2018). Multiple lines of evidence suggest a significant stratigraphic break between the Applecross Formation and the underlying Diabaig Formation (e.g., erosional discordance, sedimentary facies, mineralogy, diagenesis and organic carbon character) (Prave, 2002; Kinnaird et al., 2007; Muirhead et al., 2017; McMahon and Davies, 2018c).

3) The Aultbea Formation (1500 metres thick), which consists dominantly of medium-grained sandstones, transitions gradationally from the coarser underlying Applecross Formation. The boundary is loosely placed at points in the succession where medium-grained sandstones account for >50% of the total lithology (Stewart, 2002). As the Applecross-Aultbea succession represents one continuous phase of deposition, with the Aultbea Formation simply reflecting a facies transition (Nicholson, 1993; Stewart, 2002; Kinnaird et al., 2007), the two formations are grouped in this study and are hereafter collectively referred to as 'Torridon alluvium' (Fig. 1).

4) The Cailleach Head Formation (800-metres-thick) is interpreted as freshwater deltaic deposits (Stewart, 1988). Sedimentary facies are introduced in Section 7.3, but a more detailed sedimentary analysis of this formation is overdue.

Numerous studies have discussed the holistic sedimentary history of the Torridon Group (e.g., Selley, 1965; Williams, 1966, 2001; Stewart, 1969, 1982; Nicholson, 1993; McManus and Bajabaa, 1998), its provenance and geochemistry (e.g., Stewart, 1991; Stewart and Donnellan, 1992; Williams and Foden 2011, Krabbendam et al., 2017), and its palaeomagnetic (e.g., Stewart and Irving, 1974; Smith et al., 1983) and tectonostratigraphic (Kinnaird et al., 2007) characteristics. More recently, the succession has seen a resurgence of geobiological interest because microfossils extracted from Torridonian mudstones, first described by Teall (1907), have been recognized as Earth's oldest non-marine eukaryotes (Strother et al., 2011; Battison and Brasier, 2012) and sedimentological evidence for early microbial life on land has been described (Prave, 2002; Callow et al., 2011; Brasier et al., 2016; Strother and Wellman, 2016) (see Section 7).

The most recent comprehensive sedimentological study of the Torridon Group's entire outcrop belt was published in a Geological Society of London Memoir by Stewart (2002), summarizing over 40 years of research (e.g., Stewart, 1962, 1963, 1966, 1969, 1972, 1982, 1991; Stewart and Irving, 1974; Stewart and Parker, 1979). Stewart (2002) provided abundant information on the lithofacies

assemblages of multiple outcrop locations, but little attention was given to variations in depositional architecture, or the fact that the sedimentary system was operating in the complete absence of land plants. This paper focuses on these important aspects of the Torridon Group.

4. METHODS AND TERMINOLOGY

Data was collected from 32 sites (Fig. 1; Table 1) in the form of mapped field relationships, sedimentary logs and architectural panels, over the course of 110 field days (McMahon, 2018). Most of the studied sites have exposures suited to facies and palaeocurrent analysis. Palaeocurrents were obtained whenever reliable surfaces were available. Foreset planes were re-oriented on a stereonet to remove bedding dip whenever dip amount exceeded 10°. Techniques used to present palaeocurrent measurements follow the method described by Davies et al. (2018), whereby the scale-bar illustrated at the base of the image is the two-dimensional representation of a horizontal compass oriented to the field photograph, with arrow heads marking the obliquity of palaeoflow relative to the vertical centre-line of the image (into (upwards arrows) or out of (downward arrows) the image).

Detailed architectural element analysis (e.g., Miall, 1985) requires exposures of substantial size, which are commonly available in the Torridon outcrop belt. Observations of sedimentary structures, erosional and depositional surfaces, grain-size trends and palaeoflow dispersal directions (in sections both parallel and perpendicular to regional palaeoflow) were plotted on architectural panels in order to assess depositional architecture.

Definitions of the terms used to describe alluvium in this paper are clarified in Table 2, as some of these have been applied in contradictory ways in existing literature. A list of the architectural elements referred to is presented in Table 3. Architectural deposits were described in terms of their sedimentary facies, geometry and internal accretion surfaces. In total, 2333 palaeoflow indicators were collected from dipping cross-stratification foresets, and 270 accretion directions were collected from set and coset boundaries genetically related to a common underlying surface.

5. TORRIDON ALLUVIUM: ARCHITECTURAL DEPOSITS

Three mutually-exclusive architectural deposits have been identified as the building blocks that comprise the entirety of the c. 4.5 km-thickness of Torridon alluvium: 1) Erosionally-based cross-stratified sheets (c. 80%); 2) Inclined accretionary strata (c. 20%); and 3) Discontinuous mudstone to very-fine grained sandstone deposits (<<1%).

5.1. Erosionally-based cross-stratified sheets

Description

Erosionally-based cross-stratified sheets range in thickness from 0.4 – 4.75 metres (mean 2.46 m) (n = 145, S = 101.8) (S = Standard Deviation) (Fig. 2) and their basal erosional surfaces lack significant relief (Fig. 2A). Decreases in grain-size up-section from pebbly-sandstones in a coarse-grained sandstone matrix (and rare pebble conglomerates) (Fig. 3A) to medium-grained sandstones (Fig. 3B) are common. Granule and pebble lags (Fig. 3C) and mudstone rip-up clasts (Fig. 3D) regularly occur along the bases of thicker deposits. Deposits are composed dominantly of trough cross-stratified sets (Fig. 2C-D, Fig. 3E), with subordinate planar-tabular cross-stratified sets (Fig. 2C, Fig. 3F). Maximum trough set thickness is 105 cm (average 27 cm) and maximum planar-tabular set thickness is 80 cm (average 28 cm). Coset boundaries are planar and trend parallel to underlying erosional surfaces, distinguishing them from inclined accretionary deposits, which consist of multiple inclined cosets each truncating a common underlying surface (Section 5.2).

Thicker deposits exhibit frequent and extensive soft-sediment deformation, from mildly deformed cross-beds with oversteepened foresets and small-scale contortions (Fig. 4A-C), through to laterally-extensive chaotically folded and disturbed stratification (Fig. 4D-G), often truncated by overlying beds (Fig. 4H). Soft-sediment deformation is more abundant within erosionally-based sheets than it is in either of the other two architectural deposits: affecting approximately 55% of sand-bodies and

becoming increasingly abundant up-section (possibly due to the modal medium-sand grain-size, as is optimal for sediment liquefaction (Owen, 1987)).

Deposits are near-ubiquitously tabular, extending along depositional-strike sections for up to 350 metres (limited by available exposure) regardless of thickness (Fig. 2B). All of these deposits can therefore be categorized as 'sheet-braided' (Table 2). Channel-margins cannot be identified at outcrop, and the full lateral-extent of bounding surfaces in depositional-strike sections is limited by available exposure.

These architectural deposits most frequently occur within thick (up to 27 m) multistorey sandstone sequences (Section 5.4.1). Less frequently there is an upwards transition from erosionally-based cross-stratified sheets to inclined accretion strata (Section 5.2). Where deposits are not erosionally-truncated, original dune topography is sometimes preserved. Planform exposures of dune topography are exposed at a number of locations (Fig. 5).

Interpretation

Coarse-grained sandstones, with planar basal erosion surfaces that are lined with granule- or pebble-lags and mudstone rip-up clasts, are analogous to modern channel bedform sediments (Cant and Walker, 1976; Miall, 1996; Carling et al., 2000). The cross-bedding records sinuous- and straight-crested dunes that migrated under unidirectional lower-flow regimes. The absence of identifiable accretion surfaces, despite extensive exposures, suggests that these architectural deposits do not record in-channel barform migration, but rather the migration of bedforms which accumulated predominantly by vertical aggradation (i.e., sandy-bedforms, *sensu* Miall, 1985, 1996). Thick successions of cross-bedded deposits accumulate in the deeper parts of modern fluvial channels, and this provides an analogue for the Torridon Group facies.

We refer to these architectural deposits as 'channel-bedform deposits'. Where successive channel-bedform deposits are separated by planar erosion surfaces, we refer to these as 'multistorey channel-

bedform sequences' (Section 5.4.1). Laterally persistent erosional surfaces are most commonly associated with rivers with large channels (Hajek and Heller, 2012). Generally, channel-margins become gentler in slope (and therefore less recognisable at outcrop) with increasing channel width (Miall, 1996). Additionally, laterally mobile channels may rework pre-existing channel margins producing tabular sandstone bodies far greater in width than the original channel morphology (Friend, 1983; Hajek and Straub, 2017).

Soft-sediment deformation structures occur at different scales in Torridon alluvium and likely have different triggers. Deformation within individual cross-stratified sets (Fig. 4A-B) probably formed by flow-induced shear during deposition. Laterally extensive soft-sediment deformed horizons (Fig. 4C-F) are frequently top-truncated (Fig. 4E-F), indicating that this deformation did not occur through compaction after deposition. No evidence was uncovered here to determine the exact trigger of liquefaction but previous studies have offered a plurality of viable explanations: 1) groundwater movements (Owen and Santos, 2014); 2) flow-related turbulence (Owen, 1996); or 3) seismic activity (Owen and Santos, 2014). A seismic origin may be likely when different expressions of soft-sediment deformation (depending on lithology) occur along the same stratigraphic horizon (Davies et al., 2005). However, within Torridon alluvium, lithological monotony makes confident stratigraphic correlation between outcrops, separated by non-exposure and drift cover, impossible. Thus a seismic origin can neither be confidently determined nor conclusively ruled out.

5.2. Inclined accretionary strata

Description

Inclined accretionary strata most frequently occur above coarser, underlying channel-bedform deposits (Fig. 6). The architectural deposit consists of inclined sets and cosets of cross-stratified sandstone that are genetically related to a common underlying bounding surface (Fig. 6, Fig. 7). Maximum coset thickness is 510 cm (mean 184 cm) (n = 52, S = 107). Individual inclined sets are

predominantly planar or planar-tangential (Fig. 6), although sigmoidal geometries also occur (Fig. 7A-B, Fig 7D). Maximum planar set thickness is 160 cm (average 97 cm) (n = 36, S = 33.6) and maximum sigmoidal set thickness is 200 cm (mean 132 cm) (n = 16, S = 32.0). Infrequent low-angle cross-stratification and horizontal-laminae occur towards the top of individual deposits (Fig. 7C, Fig. 7F). Some show oversteepening by soft-sediment deformation (Fig. 7D-E). Accretion directions are varied, dipping downstream and normal to local palaeoflow (Fig. 6, Fig. 7A). Deposits are never heterolithic, but can display subtle fining- and coarsening-up profiles. Rare reactivation surfaces are marked by gravel lags.

Deposits are up to 70 metres wide in depositional-strike sections, and can be traced down depositional-dip for more than 100 metres (dimensions are constrained by available exposure in both dip and strike sections). Rarely, deposits can be seen to be overlain by fine-grained material (Section 5.3), or stack to form multistorey composite bodies (Section 5.4.1). However, they are most commonly erosively overlain by a subsequent channel-bedform deposit (Fig. 8).

Interpretation

Inclined accretionary deposits are interpreted as barform deposits, where the inclination of coset surfaces reflects barform migration (Miall, 1985; Long, 2011). The palaeoflow orientations of cross-stratification within each coset represent the migration of bedforms along the bar. Of the 262 deposits where accretion and palaeocurrent directions were available, 56% showed downstream- or downstream-lateral accretion (n=147) and 33% showed lateral accretion (n=85). Downstream- and lateral-accretion elements are the principal products of accretion within barforms of major sand-bed channels (Miall, 1996). The incremental character of inclined accretionary elements suggests periodic migration of barforms during peak flood, separated by periods of low flow (e.g., Bristow, 1987; Best et al., 2003).

Rare barform reactivation surfaces can represent falling stage modifications to the bed surface (Collinson, 1970). Upstream- and upstream-lateral accretion elements were recognised in association with these surfaces (n=30, 11%). In modern rivers, such surfaces are observed at the upstream end of large mid-channel barforms, with accretion predominantly occurring during falling flood stages (Bristow, 1987, 1993; Best et al., 2003). Such a refined assessment was not possible for Torridon alluvium as the original barforms never crop out in their entirety.

Lateral accretion is displayed more commonly in sigmoidal accretionary surfaces than it is in inclined planar accretionary surfaces, as is reflected in their mean accretion directions of 76° and 113° respectively (mean palaeoflow 126°) (Section 5.6.1). Due to the range of possible accretion directions, barform deposits in modern alluvial systems display greater flow dispersal than channel-bedform deposits. It is important to note that there were many instances where accretion directions could not be obtained at all from a suspected barform deposit: a consequence of the weathered condition of many of the rock exposures.

No channel-bedform deposits were seen to pass laterally into barform deposits. Thus there were only two instances where bank-attached bars could be interpreted; where inclined accretion surfaces were observed to dip towards, and be truncated by, fine-grained deposits (interpreted to have filled abandoned channels; see Ielpi and Ghinassi, 2015, their Figure 8). This scarcity may be due to autogenic sediment-transport dynamics, as opposed to original morphology.

5.3. Discontinuous fine-grained deposits (mudstone to very fine-grained sandstone)

Description

Discontinuous fine-grained deposits (mudstone to very fine-grained sandstone) are extremely rare, with only 14 observed examples (note that this figure does not include examples in the Allt-na-Béiste Member, which is most accurately considered to be the topmost member of the underlying Diabaig Formation; see McMahon and Davies (2018c)).

Deposits are up to 30 metres wide (Fig. 9A) and 2.4 metres thick (Fig. 9C) (mean 0.25 metres (S = 0.6)). They most often succeed barform deposits, although at three localities they overlie erosive surfaces (Fig. 9A). Mudstones and siltstones are either oxidized red (Fig. 9A) or are grey in colour (Fig. 9B-C). Horizontal laminae and ripple cross-lamination are common in coarse-grained siltstones and very fine-grained sandstones (Fig. 9D-E). Some ripple cross-laminated sandstones show soft-sediment deformation (Fig. 9E) and contain small intraformational mud clasts (Fig. 9F).

Interpretation

Mudstone to very-fine sandstone deposits are here interpreted to represent deposition on the floodplain, away from the active channel; or, more rarely, from infill of abandoned channel areas. The scarcity of these strata within Torridon Group alluvium is attributed to their propensity for reworking by active channels at the time of deposition. The relatively low bank stability would likely have meant that frequent floodplain reworking would have been commonplace in the original depositing rivers. This has been recognized in other instances where vegetation was limited or missing, including other pre-vegetation alluvium (e.g., Cotter, 1978; Hjellbakk, 1997; Gibling and Davies, 2012), numerical (Oorschot et al., 2016) and experimental models (van Dijk et al., 2013), and observations from modern, poorly vegetated rivers (Tooth, 2000).

5.4. Architectural deposit stacking patterns

The three observed architectural deposits stack to form a larger-scale hierarchy of well-defined sequences (Fig. 10), including multistorey channel-bedform deposits, channel-belts and composite barforms.

5.4.1. Multistorey channel-bedform sequences

Where the architectural deposits defined in sections 5.1 – 5.3 stack into one cycle (ascending: channel-bedform deposit, barform deposit, out-of-channel deposit), this records the migration and

384 infilling of a discrete channel, succeeded by abandonment and the establishment of floodplain
385 deposition (Allen, 1965). However, autogenic reorganisation of any fluvial system inevitably leads to
386 partial shredding of such a sedimentary record (Foreman and Straub, 2017), and it is unsurprising
387 that such ideal sequences are only very rarely observed in Torridon alluvium. Most commonly,
388 multiple channel-bedform deposits stack vertically without preserving any associated barform or
389 out-of-channel deposits (Fig. 11). In these successions, laterally-extensive, low-relief erosional
390 surfaces separate individual channel-bedform deposits. These successions are termed 'multistorey
391 channel-bedform sequences' (Fig. 10).

392 In these outcrops, multistorey channel-bedform sequences are biased in preferentially preserving
393 the topographically lowest portions of the channel (e.g., Godin, 1991; Went and McMahon, 2018).
394 Preservation of only the deepest parts of a river system is regarded as the product of aggradation co-
395 occurring with lateral channel-migration (Bluck, 1971; Miall, 1980; Todd and Went, 1991; Lewin and
396 Macklin, 2003). Lateral channel migration or combing reworks barforms and out-of-channel material
397 and enables the longer-term aggradation of several generations of channel-bedform deposits.
398 Occasionally remnant barform deposits are partially preserved amongst multistorey channel-
399 bedform sequences (Fig. 12). Similar observations have been made in other ancient sedimentary
400 succesions (e.g., McLaurin and Steel, 2007) and support the hypothesis that these are the remains of
401 numerous channel-bar systems.

402 *5.4.2. Channel-belt sequences*

403 Channel-bedform deposits or multistorey channel-bedform sequences which are succeeded by a
404 barform deposit (and rarely in turn by out-of-channel material) are described here as 'channel-belt'
405 sequences (Fig. 10, Fig. 12, Fig. 13). In these instances, deposits must have escaped reworking by
406 subsequent channel migration because the active channel-belt was transposed elsewhere through
407 avulsion (e.g., Bristow, 1996; Heller and Paola, 1996; McLaurin and Steel, 2007; Hajek and Heller,

2012). Sequences of channel-bedform deposits or multistorey channel-bedform sequences capped by a barform deposit were laid down between avulsion events and can therefore be defined as 'channel-belt' sequences (Fisk, 1944).

Crucial to this interpretation is the recognition that channel-bedform deposits record the topographically lowest portion of numerous channel-bar systems. The barforms associated with these sedimentary deposits are incompletely preserved or entirely absent because of repetitive shredding by actively migrating channels. Constraints on maximum channel-belt thickness are restricted in some instances by the inaccessibility of some large vertical successions (e.g., sea cliffs). However, Torridon alluvium also flank a number of climbable mountains (in this study: Liathach, Beinn Eighe, Ben Alligin, Seana Mhealan; Stac Pollaidh, Suilven and Quinag), enabling multiple channel-belt sequences to be detailed through their entire stratigraphic thickness. In these instances, the thicknesses of channel-belt sequences demonstrate no trend across the outcrop belt, ranging from 2.8 – 30.0 metres (mean = 10.8 metres (n = 42; S = 5.3)).

5.4.3. Composite barform sequences

At some localities, multiple stacked barform deposits crop out forming sequences up to 9 metres thick. These instances are termed 'composite barform sequences' (Fig. 10, Fig. 14).

The process responsible for barform deposit stacking in the Torridon is uncertain. Preservation of fluvial deposits is known to be affected by the relative balance between aggradation rate and available accommodation (Bristow and Best, 1993). One possible explanation is that episodes of bar-build up may relate to phases of high-aggradation (possibly during early waning-flood stages) (Ielpi and Ghinassi, 2015; Ghinassi and Ielpi, 2018) as these conditions would reduce the time available for barform reworking by channel-migration. Alternations between channel-bedform dominated, low-aggradation and barform dominated, high-aggradation phases may explain the relatively high

abundance of barform deposits in certain Torridon Group localities (e.g., Stoer, Achiltibuie) and their relatively scarcity in others (e.g., Bealach na Bà, Aultbea).

5.5. Case Study Torridon Section: Seana Mheallan

This locality is located approximately 1 km ESE south of the Torridon junction on the A896 road connecting Kinlochewe and Shieldaig (Fig. 15A). The predominantly depositional-strike section trends northeast to southwest, perpendicular to the prevailing southeastwards regional palaeoflow. The vertical profile in Figure 15E was measured along the southwest end of the outcrop (Fig. 15B), from the base of Seana Mheallan adjacent to the River Torridon, towards the mountain summit. The 237-metre-high section demonstrates the architectural hierarchy of channel-bedform, channel-bar and channel-belt sequences that typifies the entire Torridon alluvium outcrop belt.

Channel-bedform deposits dominate the succession, averaging 3.2 m thickness (n = 57). Internally, channel-bedform deposits comprise trough-cross stratification and show general fining-up trends. Barform deposits were recognized in 14 instances and reveal a number of channel-belts (Fig. 15E). Channel-belts have an average thickness of 15.6 metres, although with high individual variability (5.0 – 30.0 metres). Barforms predominantly display a low dispersal to local and regional palaeoflow (section 5.6.1), indicating net downstream accretion (Fig. 15D). Channel belts 5, 6, 9, and 12 display lateral accretion and channel-belt 14 upstream accretion. Channel belt 3 is capped by 10 cm of finer-grained (siltstone) out-of-channel material (Fig. 15C). This is the only instance of preserved out-of-channel material in the entire 237-metre-thick succession. Barforms have predominantly planar or planar-tangential geometries (Fig. 15D), although channel-belts 5 and 6 have associated sigmoidal barforms, and in both instances demonstrate lateral- and downstream-lateral modes of accretion. Composite barforms were not recognized in the Seana Mheallan section.

5.6. Interpreted characteristics of the Torridon alluvium

5.6.1. Palaeocurrent analysis

455 Palaeocurrent directions were obtained by measuring the dip directions of cross-strata foresets and
456 plotted on a regional map to assess transport patterns. Across the entire outcrop belt, mean transport
457 direction was towards 127^0 (n = 2333, S = 45.7). This is similar to the result of Nicholson (1993) who
458 calculated a mean flow towards 123^0. There is little variance in palaeocurrent direction between
459 locations, across the entire outcrop belt (Fig. 16). However, there is a far lower dispersal of
460 directional data for channel-bedform deposits than there is for accretion of barform deposits (Fig.
461 16) (n = 270, S = 83.6), reflecting the variability of potential barform accretion directions (i.e., lateral
462 and downstream). Channel-bedform deposits with and without directly overlying barform deposits
463 exhibit similar palaeoflow orientations (128° vs 127°).

464 Owen and Santos (2014) suggested that a large proportion of preserved soft-sediment deformation
465 structures formed in inactive but water-saturated areas of the fluvial system, and considered this
466 more consistent with a fluvially-dominated alluvial fan or distributive fluvial system (DFS)
467 depositional model, than the previously suggested alluvial braidplain model (Nicholson, 1993). The
468 palaeocurrent measurements do not support such an interpretation, at least at the scale shown by
469 Owen and Santos (2014) in their depositional model (their Figure 14). Identification of such a DFS in
470 the rock record is aided by the identification of a radial distribution of palaeocurrent directions (e.g.,
471 Hartley et al., 2010), yet the collected palaeocurrent directions show similar modal orientations
472 across the entire 30 km x 200 km wide outcrop belt. Although it is recognized that radial
473 palaeocurrent distributions are not a prerequisite for the identification of an ancient DFS, other
474 crucial criteria, including a decrease in channel amalgamation and channel presence downstream
475 (e.g., Weissmann et al., 2015), cannot be made in a pre-vegetation alluvial succession which preserves
476 scarce evidence of former channel-margins. This palaeocurrent arrangement neither permits the
477 interpretation of a tributive fluvial pattern, and only demonstrates that: 1) there is little change in
478 channel orientation across the outcrop belt; 2) there are few vertical changes in flow direction
479 throughout the stratigraphic succession, although younger deposits are more dominantly towards

480 the southeast. The palaeoflow direction also indicates that the original depositing rivers were flowing
481 in a direction away from the Grenvillian Mountains, formed by the assembly of the supercontinent
482 Rodinia around 1.2-1.0 Ga (Rainbird et al., 2011), supporting provenance studies that indicate a
483 Grenvillian source (see Krabbendam et al., 2017).

484 *5.6.2. Channel depth estimates*

485 Previous channel depth estimates have been calculated from dune-depth scaling relations based on
486 cross-stratification thickness (e.g., Leclair and Bridge, 2001), and have yielded formative depths of 1
487 – 16 m (Nicholson, 1993; Ielpi and Ghinassi, 2015; Ganti et al., 2019). In this study, flow depths were
488 estimated from the top of a barform deposit to the erosional base of an underlying, genetically related
489 channel-bedform deposit. Since barform deposits are most regularly top-truncated by a succeeding
490 channel-bedform deposit (Fig. 8) these estimates should be considered to be minima. The results
491 show that minimum flow depths range from 1.7 to 8.0 m (average 3.8 m, n = 33). There is also
492 evidence for an increase in average channel depth through time (Table 4), results which align with
493 those recently reported by Ganti et al. (2019). Clearly Torridon channels had the capacity to maintain
494 mature, large-scale fluvial drainage capable of transporting sediment for 10^3-10^4 kilometres (and
495 further supporting the likely Grenvillian source noted in Section 5.6.1.).

496 *5.6.3. Were there originally Torridonian floodplain deposits?*

497 Finer-grained floodplain material is scarce in the Torridon Group, and in pre-vegetation alluvium
498 generally (McMahon and Davies, 2018a). The only direct evidence for overbank fines in the
499 Applecross and Aultbea formations is found in the 14 isolated instances of discontinuous fine-grained
500 strata (Fig. 9) and rare intraformational mud clasts, which attest to mechanical reworking of fine-
501 grained sediment piles (Fig. 3D, 9D). This is perhaps unsurprising because, in modern river channels
502 that have weak banks (such as those diminished in the fortifying effects of plants), widening rather
503 than incision is the primary sedimentary response to fluctuating discharge (Wolman and Brush,

1961; Xu, 2002). Frequent shifting of channels and bars, in addition to an increased tendency for channel widening, would have had the potential to cause significant reworking of floodplain areas. In addition to inhibiting erosion, plants also increase the retention of all fine-grained material through the process of baffling, the capture and forced deposition of grains passing over and around above-ground parts of (even diminutive) plants (Gurnell, 2014; Mitchell et al., 2016).

The few instances of overbank fines that are known contain evidence that the Torridon floodplains were colonized by microbial mats: Section 7 contains details of these and a discussion of their inefficacy in stabilizing river banks.

5.6.4. Timescales of deposition

An exposure of the Applecross Formation was used by Paola et al. (2018) to illustrate the concept of stratigraphic time as preserved in the rock record. Noting that the duration of deposition of the Torridon Group was tens of millions of years, they emphasized the time-incompleteness of the unit, given that individual bed-forming sedimentary structures formed on timescales of minutes to a few hours. However, this time-incompleteness refers only to a vertical section at any one point and much 'lost time' is compensated for because the locus of deposition would have spatially-fluctuated across (and beyond) the preserved outcrop belt (Runkel et al., 2008; Reesink et al., 2015; Davies and Shillito, 2018). This lateral shuffling of stratigraphic time renders it effectively impossible to accurately time-correlate discrete exposures of rock within the group, even if the highly improbable scenario arose whereby it was possible to confirm that they shared the same stratigraphic horizon. It remains true that, at the scale of a depositional package outcrop (i.e., either a complete geomorphological exposure, or the strata contained between two erosive bounding surfaces that have a greater lateral continuity than the exposure), the sedimentation rate scales (Miall, 2015) that are recorded will be on the order of minutes to, at most, years. Each individual exposure of Torridon Group strata is thus a snapshot, of high temporal resolution, of the activity of pre-vegetation rivers during a singular

instant of 'Torridon time' (almost certainly a different short-term time interval to that recorded in any other discrete outcrop). The similarity of sedimentary signatures between outcrops, despite the extreme improbability of their contemporaneousness, is testament to the unwavering prevalence of particular fluvial conditions for extremely long intervals during the tens of millions of year it took to deposit the entire Torridon Group.

6. TORRIDON ALLUVIUM AS A PRE-VEGETATION ARCHETYPE?

Comparing characteristics of the original depositing rivers, as interpreted from alluvial signatures, with other reports of pre-vegetation alluvium from across the globe illustrates a number of archetypal pre-vegetation characteristics.

6.1. Fluvial style

Tabular, cross-stratified sheets, interpreted as channel-bedform deposits comprise over 80% of the Torridon alluvium's total 4.5 km stratigraphic thickness (Section 5.1). This dominance of tabular, 'sheet-braided' architectures (Table 2, Fig. 17) is typical of the vast majority of globally-preserved pre-vegetation alluvium (Cotter, 1978; Davies et al., 2011). Conversely, to date no alluvial succession post-dating the rise of vegetation has been described as dominantly 'sheet-braided'. The architectural style may thus represent a key separator between alluvium deposited before and after the evolution of land plants, but does not in itself imply that the original depositing rivers were braided in planform. Instead, the direct evidence that Torridon alluvium was the deposit of a dominantly low-sinuosity river system includes: 1) low palaeocurrent variance; 2) a lack of observable channel-margins; and 3) evidence for predominantly downstream accreting in-channel barforms.

It is not necessarily the case that all pre-vegetation rivers shared the dominantly low-sinuosity planform of the Torridon examples, and the abundance of sinuous planforms globally is uncertain. With fewer bank-stabilizing agents due to the lack of land plants and infrequency of cohesive sediment (McCormick and Grotzinger, 1993; Davies and Gibling, 2010; McMahon and Davies 2018a),

552 the flow resistance necessary to enable channel meanders almost certainly occurred less frequently
553 (Dietrich and Perron, 2006). However, observations of modern rivers demonstrate that bank stability
554 can also be afforded abiotically (e.g., Ferguson, 1987; Matsubara et al., 2015) such that meandering
555 river deposition should not be wholly unexpected on the pre-vegetation Earth (Davies and Gibling,
556 2010b). Despite skepticism over the use of horizontal planform as a descriptor when defining vertical
557 facies models (Bridge, 1985, 1993; Ethridge, 2011; Fielding et al., 2018), detailed sedimentological
558 analyses have recognized possible, sandy meandering river deposits from the pre-vegetation alluvial
559 record (e.g., Long, 2011). The majority of interpretations of ancient channel meanders utilize the
560 widespread occurrence of lateral-accretion packages. In addition to their previous identification at
561 the Stoer Peninsula (e.g., Ghinassi and Ielpi, 2018), such packages were recognized across the
562 Torridonian outcrop belt over the course of this study (n = 85). However, such packages are not
563 conclusively diagnostic of meandering planforms because lateral accretion can occur on the flanks of
564 mid-channel braid bars during waning flood (e.g., Best et al., 2003; Strick et al., 2018). Conversely, as
565 all rivers have a degree of variability in planview morphology (e.g., Ethridge, 2011), it is possible that
566 some of the lateral-accretion deposits recognized in this study record deposition in locally sinuous
567 channels. Recently, Ganti et al. (2019) have approached the question of Torridonian fluvial planform
568 from a different, numerical modelling, angle using a mass balance calculation. Assuming that the
569 gradients of modern and ancient rivers of different planforms are directly analogous, they combined
570 interpreted flow depths with some estimates of: 1) particle Reynolds number; 2) the bounds on the
571 range of Shields stress; 3) water discharge of Precambrian rivers; and 4) assumed average
572 precipitation rate. The palaeogradients that they derived from their estimates were analogous to the
573 gradients of modern, single-threaded meandering rivers, and they concluded that the Torridon
574 alluvium was therefore also likely the product of single-threaded, meandering rivers. Whilst such
575 models are highly quantitative, there is little empirical geological support for Ganti et al.'s (2019)
576 hypothesis: primarily because Torridon strata display a very narrow dispersal of palaeocurrent

observations across the entire 200 km wide outcrop belt and throughout the entire 4.5 km thick vertical succession (Fig. 16) – a characteristic that is apparently incompatible with meandering deposition. In light of the absence of any tangible outcrop evidence for meandering deposition, it is plausible that one or more of the parameters applied in the mass balance may have been misestimated.

6.2. Discharge regime

As has been repeatedly noted (e.g., Long, 2006; McMahon et al., 2017), notions that pre-vegetation rivers were solely characterized by sand-bodies deposited in single episodes of flooding should be rejected (*contra* Trewin, 1993; Love and Williams, 2000; Gouramanis et al., 2003; Bose et al., 2012; Mukhopadhay et al., 2014). The expected higher runoff rates in pre-vegetation times (Tirsgaard and Øxnevad, 1998) would have meant that ephemeral systems likely developed across a broader range of climate zones. Successions bearing evidence for ephemeral fluvial deposits are common (e.g., Hjellbakk, 1997; Sønderholm and Tirsgaard, 1998; McMahon and Davies, 2018b) and recognizable as stacks of individual beds, each bearing evidence of waning flood conditions and intervening intervals of sedimentary stasis (Tunbridge, 1984; Olsen, 1987; Gall et al., 2017; McMahon and Davies, 2018b). However, the global census of pre-vegetation alluvium clearly demonstrates that not all pre-vegetation rivers were ephemeral.

Extensive channel-bedform deposits and a paucity of channel margins, despite evidence of considerable water depths, suggests that the Torridon channels were laterally mobile. Numerical models of laterally mobile multi-thread channel networks have produced stratigraphic stacking patterns dominated by units with similar tabular geometries (Wang et al., 2011; Straub and Wang, 2013). Barform deposits demonstrate variable growth directions, although downstream accretion is most prevalent. The incremental character of barform deposits demonstrates that not all sand-bodies were deposited in single episodes of flooding, implying that flow may have been perennial (Long,

2006). Additionally, Torridon alluvium is dominated by stacked, lower flow regime sedimentary structures, typical of perennial fluvial flow (e.g., Bristow, 1987; Best et al., 2003). The combination of: 1) dominant cross-bedding with; 2) rarer, modified barform deposits suggests that rivers were typified by moderate values of annual peak discharge variance (Fielding et al., 2018).

Channel-bedform, multistorey channel-bedform and channel-belt thicknesses are stochastically distributed throughout the Torridon succession. The lack of systematic trends suggests cyclic controls on accommodation were not the dominant control on preserved sedimentary architecture. Minor areas of barform build-up may relate to high aggradation after flood events (Ielpi and Ghinassi, 2015; Ghinassi and Ielpi, 2018). Fluvial style varies little throughout the sedimentary succession implying sedimentation was largely undisturbed throughout Torridon alluvium's entire depositional history.

In the Torridon Group and elsewhere (e.g., Todd and Went, 1991; Long, 2006, 2011; Ielpi and Rainbird, 2015; Lowe and Arnott, 2016), the prevalence of sedimentary bodies dominated by stacked, lower flow regime, 3D sedimentary structures, combined with interpretations of large barform deposits, is strongly implicative of perennial flow (e.g., Bristow, 1987; Best et al., 2003). It is therefore clear that pre-vegetation rivers were characterized by a spectrum of discharge variations, as is reflected in the diversity of sedimentary body types preserved in the pre-vegetation alluvial rock record (see Fielding et al., 2018).

7. EVIDENCE FOR MICROBIAL LIFE FROM THE TORRIDON GROUP

There is a wealth of evidence, from microbial organic remains and sedimentary surface textures, to indicate that the Torridon landscapes were not wholly abiotic, despite the absence of vegetation (Teall, 1907; Zhang et al., 1981, Zhang 1982; Prave, 2002; Callow et al., 2011; Strother et al. 2011; Battison & Brasier 2012; Wacey et al. 2014; Wellman & Strother 2015; Strother & Wellman 2016).

In this section we describe possible microbial sedimentary surface textures from the Torridon Group, alongside thin section evidence of organic remains.

Attaining unambiguous proof of a microbial origin for an individual sedimentary surface texture from field observation alone is rarely possible, as numerous abiotic and biotic mechanisms can produce similar textures. As a result, surface textures detailed in this section are assigned a category indicating the degree of certainty of a microbial formation mechanism, following the scheme set out by Davies et al. (2016): Category B are definitively biotic (microbial) and Category A are definitively abiotic; Category Ba is assigned for structures with evidence for a biotic origin, but an abiotic origin cannot be ruled out (Ab for the converse situation); Surface textures with a plausible biotic origin, but where there is no clear evidence are Category ab.

7.1. Diabaig Formation

Shale units, which contain randomly aligned, bifurcating symmetrical ripples and abundant desiccation cracks on certain bedding planes, contain the only potential evidence for microbial life in the Diabaig Formation. Previous reports include: 1) Wrinkle structures with sharp and smooth crests, attributed to microbial mats on ephemerally wetted surfaces (Prave, 2002); 2) Reticulate (and 'elongate' reticulate) fabrics comprising interconnected positive epirelief ridges (often associated with a negative hyporelief counterpart developed on the succeeding bed) (Callow et al., 2011); 3) various discoidal fabrics, which may be the product of gas escape following biofilm decay (Callow et al., 2011; Brasier et al., 2016); and 4) positive epirelief sinuous ridges and grooves on bedding planes that have similarity to the microbially-related sedimentary surface texture 'Arumberia' (Callow et al., 2011; Brasier et al., 2016).

7.1.1. Reticulate marks (Ba)

Reticulate marks have long been recognized in the Diabaig Formation (Peach et al., 1907), and are by far the most abundantly preserved sedimentary surface texture (Fig. 18). They comprise of

interconnected positive epirelief ridges around 0.3-3 cm diameter polygons. Reticulate marks occur solely in mudstone facies, with thin mud veneers seen to drape underlying topography (Fig. 18A). On occasion, small (0.3-0.5 cm) polygons occur within larger (1-3 cm) polygons (Fig. 18B). They are only found in sections which show evidence for very-shallow water depths and frequent emergence (Callow et al., 2011).

Reticulate marks have previously been hypothesised to be the product of small-scale interactions between rainfall and microbially induced extracellular polymeric substances (Strother et al., 2011), but bear stronger resemblance to modern instances of reticulate patterns arising from the tangling of filamentous bacteria on a microbial (Shepard and Sumner, 2010) or algal (Davies et al., 2016) mat.

7.1.2. Spindle-shaped cracks (ab)

Narrow, linear to curved cracks with tapering terminations were observed in fine-grained Diabaig facies at Gairloch, Raasay and Diabaig (Fig. 19A). Similar cracks were described as 'branching spindles' and 'triple-junction bird's feet' in McMahon et al. (2016-their Fig. 1). Diabaig examples were interpreted by Callow et al. (2011) as synaeresis cracks formed during the dewatering of microbially bound muddy substrates. Whilst a microbial formation mechanism is possible (Harazim et al., 2013), such cracks may also form entirely abiotically (Allen, 1982). In this instance field observation alone is insufficient to provide unequivocal proof of origin so the cracks are classified as 'ab'.

7.1.3. Wrinkle marks (ab)

Wrinkles have many potential abiotic and microbial origins (Davies et al., 2016). Within the Diabaig Formation, wrinkles solely occur in mudstone facies (Fig. 19B). They may comprise elongate, linear patches, but show no preferred orientation or alignment.

7.1.4. Circular-elliptical impressions (ab)

Circular to elliptical impressions are no more than 2.5 cm in diameter (Fig. 19C-D). On individual bedding planes they may be isolated (Fig. 19C) or occur in distinct clusters (Fig. 19D). These impressions are likely the result of burst bubbles associated with a matground or clay veneer so are classified as 'ab'; although they do occur alongside reticulate marks [Ba].

7.1.5. 'Arumberia'-like markings (ab)

Poorly preserved ridges and grooves with occasional bifurcations were identified during this study and have previously been described as 'Arumberia-like' (Callow et al., 2011) (Fig. 19E). The structures may not be true 'Arumberia', which is primarily known from latest Precambrian to Early Cambrian strata (Bland, 1984), a stratigraphic restriction which lends support to its present interpretation as an extinct matground organism (Kolesnkikov et al., 2012; Davies et al., 2016). The Diabaig 'Arumberia' differ from those described elsewhere in the global rock record by their curvature. Whilst the examples shown by Callow et al. (2011) are frequently sinuous (their Fig. 10), Arumberia described elsewhere in the rock record are predominantly 'straight' or 'low-sinuosity' (e.g., Bland, 1984; Kumar and Pandey, 2009; Kolesnikov et al., 2012, 2015). The precise origin of the 'Arumberia-like' markings in the Diabaig Formation remains enigmatic.

7.1.6. 'Lizard-skin' texture (Ba)

Surface textures bearing resemblance to the 'lizard-skin' textures described by Eriksson et al. (2007) were identified in sections along the road connecting Torridon and Diabaig (Fig. 19F). Whilst morphologically similar to reticulate marks (Fig. 18), these structures occur in negative epirelief and have far more regular spacing. Eriksson et al. (2007) proposed these textures developed by gas-escape blistering of microbial mats, although abiotic air- or gas-escape mechanisms cannot be wholly ruled out.

7.2. Aultbea and Applecross formations

693 Evidence for microbial matgrounds is restricted to the rarely preserved out-of-channel flow deposits
694 in Torridon alluvium, rather than the more typical channel-bedform deposits. No sedimentary
695 surface textures were identified, but this is potentially a result of a scarcity of bedding planes (of the
696 14 recorded instances of out-of-channel flow deposits, only 2 examples were associated with exposed
697 bedding planes). However, petrographic thin sections of these horizons provide evidence to suggest
698 that Torridon floodplains may have supported ancient microbial mats (Fig. 20). Petrographic
699 features include organic-rich carbonaceous laminae which display cohesive behavior (Fig. 20A-B)
700 and wavy-crinkly topography (often cited as evidence for microbial mats [e.g., Gerdes and Krumbein,
701 1987; Callow et al., 2011] (Fig. 20C). Interbedded layers of clastic grains and organic-material (Fig.
702 20D) might reflect alternating deposition and sedimentary stasis. As with other examples from pre-
703 vegetation alluvium, there is no evidence of microbial stabilization of river-banks; likely because the
704 surficial cohesion provided by matgrounds did not exceed thresholds for reworking by
705 hydrodynamic processes (McMahon et al., 2017).

706 *7.3. Cailleach Head Formation*

707 The Cailleach Head Formation consists of a minimum of 15 coarsening-upwards cycles, from grey
708 shales to medium-grained red sandstones (Stewart, 1988). Stewart (1988) interpreted the shales as
709 the product of deep water muds which filled a freshwater lake, whereas the sandstone units were
710 interpreted as the product of fluvial deltas. Park et al. (2002) identified desiccation cracks near the
711 top of the formation, thereby providing evidence of emergence.

712 Organic remains have previously been found within Cailleach Head shales (Battison and Brasier,
713 2012; Brasier et al., 2017), but the following provides the first description of sedimentary surface
714 textures with possible microbial origin from the unit.

715 *7.3.1. Spindle-shaped cracks (ab)*

Linear cracks with tapering terminations were observed in a loose boulder at Cailleach Head (Fig. 21A) and are similar to the Diabaig examples (section 7.1.2). The cracks bear resemblance to those described as 'triple-junction bird's feet' in McMahon et al. (2016).

7.3.2. Positive epirelief 'domes' (ab)

Simple, positive epirelief 'domes' were identified on a loose boulder at Cailleach Head. They occur as sub-circular domes 0.2 – 0.5 cm in diameter and 0.2-0.3 cm in height. The origin of these surface textures is uncertain.

7.3.3. 'Elephant skin' texture (Ba)

The term 'elephant skin texture' has become a bucket term for many sedimentary surface textures, having been repeatedly misapplied (see Davies et al., 2016). We apply the term to the surface texture in Figure 21C, which appears to match the original description of Runnegar and Fedonkin (1992). The texture consists of a tight network of reticular grooves, with the width of individual poylgons <0.5 cm. The origin of the surface texture has been described as being microbial on numerous occasions (e.g., Gehling, 1999; Steiner and Reitner, 2001).

7.3.4. Manchuriophycus (Ba)

Poor quality examples of the sinuous shrinkage crack Manchuriophycus were identified at Cailleach Head and Gruinard Island (Fig. 21D). Cracks are up to 1 cm wide and 15 cm long. Both examples were observed on the sole of a bedding plane, in proximity to sedimentary facies suggestive of shallow water depths. Manchuriophycus have been demonstrated to arise as a result of the shrinkage of microbial mats with very high strengths and elasticity (Koehn et al. 2014). As no abiotic mechanisms is known, but cannot be wholly ruled out, they are classified here as 'Ba'.

7.4. Implications

738 The sedimentary surface textures illustrated in this study and elsewhere provide strong evidence
739 that the Torridonian landscape was inhabited by microbial life. Microbiota clearly favoured quiescent
740 sedimentary environments, such as those recorded in the stillwater facies of the Diabaig and
741 Cailleach Head formations. Their absence in the alluvial facies of the Aultbea and Applecross
742 formations, despite petrographic suggestions of their presence, indicates that microbial life was also
743 present in overbank and abandoned channel areas on riverine floodplains but that they lacked the
744 mechanical capacity to prevent those deposits being reworked by fluvial channels. This accords with
745 evidence from other pre-vegetation alluvial successions where there is evidence that surficial
746 microbial mats in overbank settings were prone to undercutting and entrainment into active
747 channels (McMahon et al., 2017).

748 **8. CONCLUSIONS**

749 The ubiquity of exposed strata within the later Proterozoic 'Torridonian Sandstones' of NW Scotland
750 not only form some of the most spectacular landscapes in Britain, but are a testament to the non-
751 uniformitarian source-to-sink character of the pre-vegetation rivers that traversed Earth's
752 landscapes for the first 90% of its history. They offer one of the best opportunities to study the record
753 of pre-vegetation rivers, as 6 kilometres stratigraphic thickness of easily accessible alluvial
754 sedimentary strata. Tabular sandstone beds and a lack of mudrock enable us to consider Torridon
755 alluvium as 'archetypal' pre-vegetation alluvium, but with characteristics specific to the deposits of
756 dominantly low-sinuosity, perennial rivers.

757 • Channel-bedform deposits, barform deposits and out-of-channel deposits combine to form a
758 three-fold architectural hierarchy in which preservation is controlled by autogenic
759 readjustments.

760 • Channel-bedform deposits are the dominant component of Torridon stratigraphy and are the
761 product of laterally migrating channels under low rates of aggradation. This repetitive

process likely eroded many barforms, leaving only the topographically lowest part of the channel system preserved in the geological record. Multiple, successive channel-bedform deposits are occasionally capped by a single barform deposit, which in turn are rarely capped by out-of-channel material.

- The recognition of barform deposits suggests that occasional avulsion occurred, leaving the barform deposit less prone to erosion. Rare instances of stacked barform deposits may relate to intervals of high rates of aggradation.

- Out-of-channel deposits are rare because they had a high propensity to be reworked by the river channels. There is petrographic evidence to suggest that there was microbial life on the Torridon floodplains – an assertion backed by potential microbial signals in both the underlying and overlying formations of the Torridon alluvium. However, while they occupied some of the same physical environmental niches as later plants would, these microbial mat communities were physiologically unsuited to buffer against inevitable reworking by laterally mobile channels.

ACKNOWLEDGEMENTS

We thank the editor, Tom Challands, and the reviewers, Amanda Owen and Steven Andrews, for their helpful comments on this manuscript. WJM was supported by Shell International Exploration and Production B.V under Research Framework agreement PT38181.

References

Allen, J.R.L. 1964. Studies in fluviatile sedimentation: six cyclothems from the Lower Old Red Sandstone, Anglowelsh Basin. *Sedimentology*, ***3***, 163-198.

Allen, J.R. 1965. A review of the origin and characteristics of recent alluvial sediments. *Sedimentology*, ***5***, 89-191.

785 Allen, J.R.L. 1982. *Sedimentary Structures: Their Character and Physical Basis.* Elsevier, Amsterdam.

786 Battison, L. & Brasier, M.D. 2012. Remarkably preserved prokaryote and eukaryote microfossils
787 within 1 Ga-old lake phosphates of the Torridon Group, NW Scotland. *Precambrian Research, **196***,
788 204–217.

789 Best, J.L., Ashworth, P.J., Bristow, C.S. & Roden, J. 2003. Three-dimensional sedimentary architecture
790 of a large, mid-channel sand braid bar, Jamuna River, Bangladesh. *Journal of Sedimentary Research,*
791 ***73***, 516–530.

792 Bland, B.H. 1984. Arumberia Glaessner & Walter, a review of its potential for correlation in the region
793 of the Precambrian-Cambrian boundary. *Geol. Mag. **121***, 625–633.

794 Bluck, B.J. 1971. Sedimentation in the meandering River Endrick. *Scottish Journal of Geology*, ***7***, 93-
795 138.

796 Bose, P.K., Eriksson, P.G., Sarkar, S., Wright, D.T., Samanta, P., Mukhopadhyay, S., Mandal, S., Banerjee,
797 S. & Altermann, W. 2012. Sedimentation patterns during the Precambrian: a unique record?. *Marine*
798 *and Petroleum Geology*, ***33***, 34-68.

799 Brasier, A.T., Culwick, T., Battison, L., Callow, R.H.T. & Brasier, M.D. 2016. Evaluating evidence from
800 the Torridonian Supergroup (Scotland, UK) for eukaryotic life on land in the Proterozoic. *In*: Brasier,
801 A.T., McIlroy, D. & McLoughlin, N. (eds) *Earth System Evolution and Early Life: A Celebration of the*
802 *Work of Martin Brasier. Geological Society, London, Special Publications, **448**,* 121–144.

803 Bridge, J.S. 1985. Paleochannel Patterns Inferred From Alluvial Deposits: A Critical Evaluation
804 Perspective: Perspective. *Journal of Sedimentary Research*, ***55***, 579-589

805 Bridge, J.S. 1993. The interaction between channel geometry, water flow, sediment transport and
806 deposition in braided rivers. *Geol. Soc. London Spec. Publ. **75***, 13–71.

Bristow, C.S. 1987, Brahmaputra River: Channel migration and deposition. *In*: Ethridge, F.G., Flores, R.M. and Harvey, M.D. (ed). *Recent Developments in Fluvial Sedimentology: Contributions from the Third International Fluvial Sedimentology Conference: SEPM (Society for Sedimentary Geologists), Special Publication,* ***39***, 63–74.

Bristow, C.S. 1993. Sedimentary structures exposed in bar tops in the Brahmaputra River, Bangladesh. *Geological Society, London, Special Publications*, ***75***, 277-289.

Bristow, C. 1996. Reconstructing fluvial channel morphology from sedimentary sequences. *In*: Carling, P.A., Dawson, M.R. (eds). *Advances in Fluvial Dynamics and Stratigraphy. John Wiley & Sons, Ltd*., 351–371

Bristow, C.S. & Best, J.L. 1993. Braided rivers: perspectives and problems. *Geological Society, London, Special Publications*, ***75***, 1-11.

Callow, R.H., Battison, L. and Brasier, M.D., 2011. Diverse microbially induced sedimentary structures from 1 Ga lakes of the Diabaig Formation, Torridon Group, northwest Scotland. Sedimentary Geology, 239(3-4), pp.117-128.

Cant, D.J. & Walker, R.G. 1976. Development of a braided-fluvial facies model for the Devonian Battery Point Sandstone, Quebec. *Canadian Journal of Earth Sciences,* ***13***, 102-119.

Carling, P.A., Golz, E., Orr, H.G. & Radecki-Pawlik, A. 2000. The morphodynamics of fluvial sand dunes in the River Rhine, near Mainz, Germany. I. Sedimentology and morphology. *Sedimentology,* ***47***, 227-252.

Collinson, J.D. 1970. Bedforms of the Tana river, Norway. *Geografiska Annaler. Series A. Physical Geography*, 31-56.

828 Corenblit, D., Tabacchi, E., Steiger, J. and Gurnell, A.M., 2007. Reciprocal interactions and adjustments
829 between fluvial landforms and vegetation dynamics in river corridors: a review of complementary
830 approaches. *Earth-Science Reviews*, *84*(1-2), pp.56-86.

831 Corenblit, D., Steiger, J., Gurnell, A.M., Tabacchi, E. and Roques, L., 2009. Control of sediment dynamics
832 by vegetation as a key function driving biogeomorphic succession within fluvial corridors. *Earth*
833 *Surface Processes and Landforms, **34**,* 1790-1810.

834 Cotter, E. 1978. The evolution of fluvial style, with special reference to the central Appalachian
835 Paleozoic. *In*: Miall, A.D. (ed), *Fluvial Sedimentology: Canadian Society of Petroleum Geologists Memoir*,
836 ***5***, 361–383.

837 Dalrymple, R.W., Narbonne, G.M. & Smith, L. 1985. Eolian action and the distribution of Cambrian
838 shales in North America. *Geology*, ***13***, 607-610.

839 Davies, N.S. & Gibling, M.R. 2010a. Cambrian to Devonian evolution of alluvial systems: the
840 sedimentological impact of the earliest land plants. *Earth-Science Reviews*, ***98***, 171-200.

841 Davies, N.S. & Gibling, M.R., 2010b. Paleozoic vegetation and the Siluro-Devonian rise of fluvial lateral
842 accretion sets. *Geology, **38**,* 51-54.

843 Davies, N.S. and Shillito, A.P., 2018. Incomplete but intricately detailed: The inevitable preservation
844 of true substrates in a time-deficient stratigraphic record. *Geology, **46**,* 679-682.

845 Davies, N.S., Gibling, M.R., McMahon, W.J., Slater, B.J., Long, D.G., Bashforth, A.R., Berry, C.M., Falcon-
846 Lang, H.J., Gupta, S., Rygel, M.C. and Wellman, C.H., 2017. Discussion on 'Tectonic and environmental
847 controls on Palaeozoic fluvial environments: reassessing the impacts of early land plants on
848 sedimentation' Journal of the Geological Society, London, https://doi. org/10.1144/jgs2016-063.
849 *Journal of the Geological Society, **174**,* 947-950.

Davies, N.S., Gibling, M.R. & Rygel, M.C., 2011. Alluvial facies evolution during the Palaeozoic greening of the continents: case studies, conceptual models and modern analogues. *Sedimentology, **58**,* 220-258.

Davies, N.S., Liu, A.G., Gibling, M.R. & Miller, R.F. 2016. Resolving MISS conceptions and misconceptions: A geological approach to sedimentary surface textures generated by microbial and abiotic processes. *Earth-Science Reviews, **154***, 210–246.

Davies, N.S., McMahon, W.J. and Shillito, A.P., 2018. A Graphic Method For Depicting Horizontal Direction Data On Vertical Outcrop Photographs. *Journal of Sedimentary Research*, *88*(4), pp.516-521.

Davies, N.S., Turner, P. & Sansom, I.J. 2005. Soft-sediment deformation structures in the Late Silurian Stubdal Formation: the result of seismic triggering. *Norwegian Journal of Geology, **85,*** 233-243.

de Almeida, R.P., Marconato, A., Freitas, B.T. & Turra, B.B., 2016. The ancestors of meandering rivers. *Geology, **44**,* 203-206.

Dietrich, W.E. and Perron, J.T., 2006. The search for a topographic signature of life. *Nature, **439**,* 411-418.

Dott, Jr, R.H. 2003. The importance of eolian abrasion in supermature quartz sandstones and the paradox of weathering on vegetation-free landscapes. *The Journal of Geology*, ***111***, 387-405.

Dott Jr., R.H. & Byers, C.W. 1981. SEPM research conference on modern shelf and ancient cratonic sedimentation — the orthoquartzite-carbonate suite revisited. *Journal of Sedimentary Petrology*, ***51***, 329–347.

Edwards, D., Cherns, L. and Raven, J.A., 2015. Could land-based early photosynthesizing ecosystems have bioengineered the planet in mid-Palaeozoic times?. *Palaeontology*, *58*(5), pp.803-837.

871 Els, B.G. 1998. The auriferous late Archaean sedimentation systems of South Africa: unique palaeo-
872 environmental conditions?. *Sedimentary Geology*, ***120***, 205-224.

873 Eriksson, P.G., Porada, H., Banerjee, S., Bouougri, E., Sarkar, S., Bumby, A.J., 2007b. Matdestruction

874 features. In: Schieber, J., Bose, P.K., Eriksson, P.G., Banjeree, S., Sarkar, S., Altermann, W., Catuneau, O.
875 (Eds.), Atlas of microbial mat features preserved within the clastic rock record. Elsevier, Amsterdam,
876 pp. 76–105.

877 Eriksson, K.A. & Simpson, E.L., 1998. Controls on spatial and temporal distribution of Precambrian
878 eolianites. *Sedimentary Geology*, **120**, 275-294.

879 Ethridge, F.G. 2011. Interpretation of ancient fluvial channel deposits: review and recommendations.
880 *In*: Davidson, S., Leleu, S., North, C.P. (eds), *From River to Rock Record: The Preservation of Fluvial*
881 *Sediments and their Subsequent Interpretation*. *SEPM*, ***97***, 9-35.

882 Ferguson, R.I., 1987. Hydraulic and sedimentary controls of channel pattern. *River channels:*
883 *Environments and processes*, pp.129-158.

884 Fielding, C.R. 2006. Upper flow regime sheets, lenses and scour fills: extending the range of
885 architectural elements for fluvial sediment bodies. *Sedimentary Geology*, ***190***, 227-240.

886 Fielding, C.R., Alexander, J. and Allen, J.P., 2018. The role of discharge variability in the formation and
887 preservation of alluvial sediment bodies. *Sedimentary Geology*, *365*, pp.1-20.

888 Fisk, H.N. 1944. Geological Investigation of the Alluvial Valley of the Lower Mississippi River.
889 *Mississippi River Commission, Vicksburg, Mississippi.*

890 Foreman, B.Z. & Straub, K.M., 2017. Autogenic geomorphic processes determine the resolution and
891 fidelity of terrestrial paleoclimate records. *Science Advances, **3**,* p.e1700683.

892 Friend, P,F. 1983. Towards the field classification of alluvial architecture or sequence. *In*: J.D,
893 Collinson and J. Lewin (ed), *Modern and Ancient Fluvial Systems. Int. Assoc. Sediment. Spec. Publ.,* ***6***,
894 345-354.

895 Fuller, A.O. 1985. A contribution to the conceptual modelling of pre-Devonian fluvial systems. *South*
896 *African Journal of Geology*, **88**, 189-194.

897 Gall, R.D., Birgenheier, L.P. & Berg, M.D.V. 2017. Highly Seasonal and Perennial Fluvial Facies:
898 Implications For Climatic Control On the Douglas Creek and Parachute Creek Members, Green River
899 Formation, Southeastern Uinta Basin, Utah, USA. *Journal of Sedimentary Research*, ***87***, 1019-1047.

900 Ganti, V., Whittaker, A.C., Lamb, M.P., Fischer, W.W. 2019. Low-gradient, single-threaded rivers prior
901 to greening of the continents. *Proceedings of the National Academy of Sciences.*
902 *doi.org/10.1073/pnas.1901642116*

903 Gehling, J.G. 1999. Microbial mats in terminal Proterozoic siliciclastics; Ediacaran death masks.
904 *Palaios,* ***14***, 40–57.

905 Gerdes, G., Krumbein, W.E. 1987. Biolaminated Deposits. *Lecture Notes in Earth Sciences,* ***9***, 183.
906 Springer, New York.

907 Ghinassi, M. & Ielpi, A. 2018. Precambrian snapshots: Morphodynamics of Torridonian fluvial braid-
908 bars revealed by three-dimensional photogrammetry and outcrop sedimentology. Sedimentology,
909 65, 492-516

910 Gibling, M.R. & Davies, N.S. 2012. Palaeozoic landscapes shaped by plant evolution. *Nature Geoscience*,
911 ***5***, 99-105.

912 Godin, P. 1991. Fining-upwards cycles in the sandy-braided river deposits of the Westwater Canyon
913 Member (Upper Jurassic), Morrison Formation, New Mexico. *Sedimentary Geology,* ***70***, 61–82.

914 Gouramanis, C., Webb, J.A. & Warren, A.A., 2003. Fluviodeltaic sedimentology and ichnology of part
915 of the Silurian Grampians Group, western Victoria. *Australian Journal of Earth Sciences*, ***50***, 811-825.

916 Gurnell, A., 2014. Plants as river system engineers. *Earth Surface Processes and Landforms*, *39*(1),
917 pp.4-25.

918 Hadlari, T., Rainbird, R.H. & Donaldson, J.A. 2006. Alluvial, eolian and lacustrine sedimentology of a
919 Paleoproterozoic half-graben, Baker Lake Basin, Nunavut, Canada. *Sedimentary Geology*, ***190***, 47-70.

920 Hajek, E.A. & Heller, P.L. 2012. Flow-depth scaling in alluvial architecture and nonmarine sequence
921 stratigraphy: example from the Castlegate Sandstone, central Utah, USA. *Journal of Sedimentary*
922 *Research*, ***82***, 121-130.

923 Hajek, E.A. & Straub, K.M. 2017. Autogenic sedimentation in clastic stratigraphy. *Annual Review of*
924 *Earth and Planetary Sciences, **45***, 681-709

925 Harazim, D., Callow, R.H. & Mcilroy, D., 2013. Microbial mats implicated in the generation of
926 intrastratal shrinkage ('synaeresis') cracks. *Sedimentology, **60***, 1621–1638.

927 Hartley, A.J., Owen, A., Weissmann, G.S. and Scuderi, L., 2018. Modern and ancient amalgamated sandy
928 meander-belt deposits: recognition and controls on development. *Fluvial meanders and their*
929 *sedimentary products in the rock record (IAS SP 48)*, *48*, pp.349-384.

930 Hartley, A.J., Weissmann, G.S., Nichols, G.J. & Warwick, G.L. 2010. Large distributive fluvial systems:
931 characteristics, distribution, and controls on development. *Journal of Sedimentary Research*, ***80***, 167-
932 183.

933 Heller, P.L. & Paola, C. 1996. Downstream changes in alluvial architecture: an exploration of controls
934 on channel-stacking patterns. *Journal of Sedimentary Research, **66***, 297-306.

935 Hjellbakk, A. 1997. Facies and fluvial architecture of a high-energy braided river: the Upper
936 Proterozoic Seglodden Member, Varanger Peninsula, northern Norway. *Sedimentary Geology*, ***114***,
937 131-161.

938 Horton, A.J., Constantine, J.A., Hales, T.C., Goossens, B., Bruford, M.W. and Lazarus, E.D., 2017.
939 Modification of river meandering by tropical deforestation. *Geology, **45**,* 511-514.

940 Ielpi, A. & Ghinassi, M. 2015. Planview style and palaeodrainage of Torridonian channel belts:
941 Applecross Formation, Stoer Peninsula, Scotland. Sedimentary Geology, 325, 1-16.

942 Ielpi, A., Ghinassi, M., Rainbird, R.H. and Ventra, D., 2018. Planform sinuosity of Proterozoic rivers: A
943 craton to channel-reach perspective. *Fluvial meanders and their sedimentary products in the rock*
944 *record (IAS SP 48)*, *48*, pp.81-118.

945 Ielpi, A. and Rainbird, R.H., 2015. Architecture and morphodynamics of a 1· 6 Ga fluvial sandstone:
946 Ellice Formation of Elu Basin, Arctic Canada. *Sedimentology*, *62*(7), pp.1950-1977.

947 Ielpi, A. and Rainbird, R.H., 2016. Reappraisal of Precambrian sheet-braided rivers: Evidence for 1· 9
948 Ga deep-channelled drainage. Sedimentology, 63(6), pp.1550-1581.

949 Ielpi, A., Rainbird, R.H., Ventra, D. & Ghinassi, M., 2017. Morphometric convergence between
950 Proterozoic and post-vegetation rivers. *Nature communications*, ***8***, 15250.
951 https://doi.org/10.1038/ncomms15250.

952 Kaiser, E. 1931. Der Grundsatz des Aktualismus in der Geologie. *Zeitschrift der Deutschen*
953 *Geologischen Gesellschaft*, 389-407.

954 Kinnaird, T.C., Prave, A.R., Kirkland, C.L., Horstwood, M., Parrish, R. & Batchelor, R.A. 2007. The late
955 Mesoproterozoic–early Neoproterozoic tectonostratigraphic evolution of NW Scotland: the
956 Torridonian revisited. Journal of the Geological Society, 164, 541-551.

957 Kleinhans, M.G., de Vries, B., Braat, L. and van Oorschot, M., 2018. Living landscapes: Muddy and
958 vegetated floodplain effects on fluvial pattern in an incised river. Earth surface processes and
959 landforms, 43(14), pp.2948-2963.

960 Koehn, D., Bons, P., Montenari, M. & Seilacher, A. 2014. The elastic age: rise and fall of Precambrian
961 biomat communities. *In*: *EGU General Assembly Conference Abstracts, Abstract 16, Vienna*, EGU2014-
962 13793.

963 Kolesnikov, A.V., Grazhdankin, D.V., Maslov, A.V., 2012. Arumberia-type structures in the Upper
964 Vendian of the Urals. In Doklady Earth Sciences (Vol. 447, No. 1, pp. 1233-1239). SP MAIK
965 Nauka/Interperiodica.

966 Kolesnikov, A.V., Marusin, V.V., Nagovitsin, K.E., Maslov, A.V., Grazhdankin, D.V., 2015. Ediacaran
967 biota in the aftermath of the Kotlinian Crisis: Asha Group of the South Urals. Precambrian Research
968 263, 59-78.

969 Krabbendam, M., Bonsor, H., Horstwood, M.S. & Rivers, T. 2017. Tracking the evolution of the
970 Grenvillian foreland basin: Constraints from sedimentology and detrital zircon and rutile in the
971 Sleat and Torridon groups, Scotland. Precambrian Research, 295, 67-89.

972 Kumar, S., Pandey, S.K., 2009. Note on the occurrence of Arumberia banksi and associated fossils from
973 the Jodhpur Sandstone, Marwar Supergroup, Western Rajasthan. Journal of the Palaeontological
974 Society of India 54, 171.

975 Leclair, S.F. & Bridge, J.S. 2001. Quantitative interpretation of sedimentary structures formed by river
976 dunes. *Journal of Sedimentary Research*, ***71***, 713-716.

977 Lewin, J. & Macklin, M.G. 2003. Preservation potential for Late Quaternary river alluvium. *Journal of*
978 *Quaternary Science*, ***18***, 107-120.

Lindsey, K.A. & Gaylord, D.R. 1992. Fluvial, coastal, nearshore, and shelf deposition in the Upper Proterozoic (?) to Lower Cambrian Addy Quartzite, northeastern Washington. *Sedimentary Geology*, ***77***, 15-35.

Long, D.G. 1978. Proterozoic stream deposits: some problems of recognition and interpretation of ancient sandy fluvial systems. *In*: Miall, A.D. (ed), *Fluvial Sedimentology: Canadian Society of Petroleum Geologists Memoir*, ***5***, 313-341.

Long, D.G. 2006. Architecture of pre-vegetation sandy-braided perennial and ephemeral river deposits in the Paleoproterozoic Athabasca Group, northern Saskatchewan, Canada as indicators of Precambrian fluvial style. *Sedimentary Geology*, ***190***, 71-95.

Long, D.G.F. 2011. Architecture and depositional style of fluvial systems before land plants: a comparison of Precambrian, early Paleozoic and modern river deposits. *In*: Davidson, S., Leleu, S. & North, C.P. (eds), *From River to Rock Record: The Preservation of Fluvial Sediments and their subsequent Interpretation. SEPM*, 37–61.

Long, D.G., 2018. Archean fluvial deposits: A review. *Earth-Science Reviews*.

Love, S.E. & Williams, B.P. 2000. Sedimentology, cyclicity and floodplain architecture in the Lower Old Red Sandstone of SW Wales. *Geological Society, London, Special Publications*, ***180***, 371-388.

Lowe, D.G. & Arnott, R.W.C. 2016. Composition and Architecture of Braided and Sheetflood-Dominated Ephemeral Fluvial Strata. *In*: the Cambrian–Ordovician Potsdam Group: A Case Example of the Morphodynamics of Early Phanerozoic Fluvial Systems and Climate. *Journal of Sedimentary Research*, ***86***, 587-612.

MacCulloch, J., 1819. A Description of the Western Islands of Scotland, Including the Isle of Man: Comprising an Account of Their Geological Structure; with Remarks on the Agriculture, Scenery and Antiquities (Vol. 2). Archibald Constable and Company, Edinburgh;[&c.].

1002 MacNaughton, R.B., Dalrymple, R.W. & Narbonne, G.M. 1997. Early Cambrian braid-delta deposits,
1003 Mackenzie Mountains, north-western Canada. *Sedimentology*, ***44***, 587-609.

1004 Marconato, A., de Almeida, R.P., Turra, B.B. & dos Santos Fragoso-Cesar, A.R. 2014. Pre-vegetation
1005 fluvial floodplains and channel-belts in the Late Neoproterozoic–Cambrian Santa Bárbara group
1006 (Southern Brazil). *Sedimentary Geology,* ***300***, 49–61.

1007 Matsubara, Y., Howard, A.D., Burr, D.M., Williams, R.M., Dietrich, W.E. & Moore, J.M. 2015. River
1008 meandering on Earth and Mars: A comparative study of Aeolis Dorsa meanders, Mars and possible
1009 terrestrial analogs of the Usuktuk River, AK, and the Quinn River, NV. *Geomorphology*, ***240***, 102-120.

1010 McLaurin, B.T. & Steel, R.J. 2007. Architecture and origin of an amalgamated fluvial sheet sand, lower
1011 Castlegate Formation, Book Cliffs, Utah. *Sedimentary Geology,* ***197***, 291-311.

1012 McMahon, S., Bosak, T., Grotzinger, J.P., Milliken, R.E., Summons, R.E., Daye, M., Newman, S.A.,
1013 Fraeman, A., Williford, K.H. and Briggs, D.E.G., 2018. A Field Guide to Finding Fossils on Mars. Journal
1014 of Geophysical Research: Planets.

1015 McMahon, S., van Smeerdijk Hood, A. and McIlroy, D., 2017. The origin and occurrence of subaqueous
1016 sedimentary cracks. Geological Society, London, Special Publications, 448(1), pp.285-309.

1017 McMahon, W.J., 2018. Pre-vegetation alluvium: Geological evidence for river behaviour in the absence
1018 of land plants. Doctoral dissertation, University of Cambridge. https://doi.org/10.17863/CAM.23566

1019 McMahon, W.J. and Davies, N.S., 2018a. Evolution of alluvial mudrock forced by early land plants.
1020 *Science*, ***359***, 1022-1024.

1021 McMahon, W.J. and Davies, N.S., 2018b. High-energy flood events recorded in the Mesoproterozoic
1022 Meall Dearg Formation, NW Scotland; their recognition and implications for the study of pre-
1023 vegetation alluvium. *Journal of the Geological Society*, *175*(1), pp.13-32.

McMahon, W.J. and Davies, N.S., 2018c. The shortage of geological evidence for pre-vegetation meandering rivers. *Fluvial Meanders and Their Sedimentary Products in the Rock Record*, pp.119-148.

McMahon, W.J., Davies, N.S. and Went, D.J., 2017. Negligible microbial matground influence on pre-vegetation river functioning: Evidence from the Ediacaran-Lower Cambrian Series Rouge, France. *Precambrian Research*, *292*, pp.13-34.

McManus, J. & Bajabaa, S. 1998. The importance of air escape processes in the formation of dish-and-pillar and teepee structures within modern and Precambrian fluvial deposits. *Sedimentary Geology,* ***120****,* 337–343.

McPherson, J.G., Shanmugam, G. & Moiola, R.J. 1987. Fan-deltas and braid deltas: varieties of coarse-grained deltas. *Geological Society of America Bulletin*, ***99***, 331-340.

Miall, A.D. 1980. Cyclicity and the facies model concept in fluvial deposits. *Bulletin of Canadian Petroleum Geology*, ***28***, 59-80.

Miall, A.D. 1985. Architectural-element analysis: a new method of facies analysis applied to fluvial deposits. *Earth-Science Reviews*, ***22***, 261-308.

Miall, A.D. 1996. *The geology of fluvial deposits: sedimentary facies, basin analysis, and petroleum geology*. Springer.

Miall, A.D., 2015, Updating uniformitarianism: stratigraphy as just a set of 'frozen accidents'. *Geological Society, London, Special Publications,* ***404****,* 11-36.

Mitchell, R.L., Cuadros, J., Duckett, J.G., Pressel, S., Mavris, C., Sykes, D., Najorka, J., Edgecombe, G.D. and Kenrick, P., 2016. Mineral weathering and soil development in the earliest land plant ecosystems. *Geology,* ***44****,* 1007-1010.

1045 Muirhead, D.K., Parnell, J., Spinks, S. & Bowden, S.A. 2017. Characterization of organic matter in the
1046 Torridonian using Raman spectroscopy. Geological Society, London, Special Publications, 448, 71-80.

1047 Mukhopadhyay, S., Choudhuri, A., Samanta, P., Sarkar, S. & Bose, P.K., 2014. Were the hydraulic
1048 parameters of Precambrian rivers different?. *Journal of Asian Earth Sciences*, ***91***, 289-297.

1049 Nicholson, P.G. 1993. A basin reappraisal of the Proterozoic Torridon Group, northwest Scotland. In:
1050 Frostick, L.E. & Steel, R.J (eds). Tectonic Controls and Signatures in Sedimentary Successions, Special
1051 Publication of the International Association of Sedimentologists, 20, 183-202.

1052 Olsen, H. 1987. Ancient ephemeral stream deposits: a local terminal fan model from the Bunter
1053 Sandstone Formation (L. Triassic) in the Tønder-3,-4 and-5 wells, Denmark. *In*: Frostick, R.I (eds).
1054 *Desert Sediments: Ancient and Modern*. Geological Society of London: London; Special Publication, ***35***,
1055 69–86.

1056 Oorschot, M.V., Kleinhans, M., Geerling, G. and Middelkoop, H., 2016. Distinct patterns of interaction
1057 between vegetation and morphodynamics. *Earth Surface Processes and Landforms*, *41*(6), pp.791-
1058 808.

1059 Owen, G. 1987. Deformation processes in unconsolidated sands. *Geological Society, London, Special*
1060 *Publications,* ***29***, 11-24.

1061 Owen, G. 1996. Experimental soft-sediment deformation: structures formed by the liquefaction of
1062 unconsolidated sands and some ancient examples. *Sedimentology*, ***43***, 279-293.

1063 Owen, G. & Santos, M.G. 2014. Soft-sediment deformation in a pre-vegetation river system: the
1064 Neoproterozoic Torridonian of NW Scotland. *Proceedings of the Geologists' Association*, ***125***, 511-523.

1065 Paola, C., Ganti, V., Mohrig, D., Runkel, A.C., and Straub, K.M., 2018, Time not our time: Physical
1066 controls on the preservation and measurement of geologic time. *Annual Review of Earth and*
1067 *Planetary Sciences,* ***46,*** 409-438.

1068 Park, R.G., Stewart, A.D. & Wright, D.T. 2002. The Hebridean terrane. *In*: Trewin, N.H. (ed) *The Geology*
1069 *of Scotland. 4th edn. Geological Society, London,* 45–80.

1070 Peach, B.N., Horne, J., Gunn, W., Clough, C.T., Hinxman, L.W. & Teall, J.J.H. 1907. *The geological*
1071 *structure of the northwest highlands of Scotland.* Memoirs of the Geological Survey of Scotland.

1072 Prave, A.R. 2002. Life on land in the Proterozoic: evidence from the Torridonian rocks of northwest
1073 Scotland. Geology, 30, 811-814.

1074 Rainbird, R.H. 1992. Anatomy of a large-scale braid-plain quartzarenite from the Neoproterozoic
1075 Shaler Group, Victoria Island, Northwest Territories, Canada. *Canadian Journal of Earth Sciences*, ***29***,
1076 2537-2550.

1077 Rainbird, R., Cawood, P. and Gehrels, G., 2011. The great Grenvillian sedimentation episode: record
1078 of supercontinent Rodinia's assembly. Tectonics of sedimentary basins: recent advances, pp.583-601.

1079 Rainbird, R.H., Rayner, N.M., Hadlari, T., Heaman, L.M., Ielpi, A., Turner, E.C. and MacNaughton, R.B.,
1080 2017. Zircon provenance data record the lateral extent of pancontinental, early Neoproterozoic
1081 rivers and erosional unroofing history of the Grenville orogen. *GSA Bulletin*, *129*(11-12), pp.1408-
1082 1423.

1083 Reesink, A.J.H., Van den Berg, J.H., Parsons, D.R., Amsler, M.L., Best, J.L., Hardy, R.J., Orfeo, O. and
1084 Szupiany, R.N., 2015. Extremes in dune preservation: Controls on the completeness of fluvial
1085 deposits. *Earth-Science Reviews,* ***150****,* 652-665.

1086 Rodd, J.A. & Stewart, A.D. 1992. Geochemistry, weathering and diagenesis of the Diabaig Formation
1087 (Torridon Group) in NW Scotland. Scottish Journal of Geology, 28, 27-35.

1088 Rubinstein, C.V., Gerrienne, P., de la Puente, G.S., Astini, R.A. and Steemans, P., 2010. Early Middle
1089 Ordovician evidence for land plants in Argentina (eastern Gondwana). *New Phytologist*, *188*(2),
1090 pp.365-369.

Runkel, A.C., Miller, J.F., McKay, R.M., Palmer, A.R. and Taylor, J.F., 2008, The record of time in cratonic interior strata: does exceptionally slow subsidence necessarily result in exceptionally poor stratigraphic completeness? *Geological Association of Canada Special Paper, **48**,* 341-362.

Runnegar, B.N., Fedonkin, M.A., 1992. Proterozoic metazoan body fossils. *In*: Schopf, J.W. & Klein, C. (eds), *The Proterozoic Biosphere: A Multidisciplinary Study. Cambridge University Press*, 369–388.

Russell, R.J. 1956. Environmental changes through forces independent of man. *In*: Thomas, W.L. (ed). *Man's role in changing the face of the earth: Chicago, Univ. Chicago Press,* 453-470.

Santos, M.G., Almeida, R.P., Godinho, L.P., Marconato, A. & Mountney, N.P. 2014. Distinct styles of fluvial deposition in a Cambrian rift basin. *Sedimentology*, ***61***, 881-914.

Santos, M.G. & Owen, G. 2016. Heterolithic meandering-channel deposits from the Neoproterozoic of NW Scotland: Implications for palaeogeographic reconstructions of Precambrian sedimentary environments. *Precambrian Research*, ***272***, 226-243.

Santos, M.G., Hartley, A.J., Mountney, N.P., Peakall, J., Owen, A., Merino, E.R. and Assine, M.L., 2019. Meandering rivers in modern desert basins: Implications for channel planform controls and prevegetation rivers. Sedimentary Geology, 385, pp.1-14.

Schumm, S.A. 1968. Speculations concerning paleohydrologic controls of terrestrial sedimentation. *Geological Society of America Bulletin*, ***79***, 1573-1588.

Sedgwick, A. & Murchison, R.I. 1829. On the structure and the relations of the deposits constrained between the Primary rocks and the Oolitic Series in the north of Scotland. *Transactions of the Geological Society of London, 2nd Series,* ***3*****,** 125–160,

Selley, R.C. 1965. Diagnostic characters of fluviatile sediments of the Torridonian formation (Precambrian) of northwest Scotland. *Journal of Sedimentary Research, **35***, 366–380.

1113 Shepard, R.N. & Sumner, D.Y. 2010. Undirected motility of filamentous cyanobacteria produces
1114 reticulate mats. *Geobiology, **8***, 179–190.

1115 Smith, R.L., Stearn, J.E.F. & Piper, J.D.A. 1983. Palaeomagnetic studies of the Torridonian sediments,
1116 NW Scotland. *Scottish Journal of Geology, **19**,* 29–45.

1117 Sønderholm, M. & Tirsgaard, H. 1998. Proterozoic fluvial styles: response to changes in
1118 accommodation space (Rivieradal sandstones, eastern North Greenland). *Sedimentary Geology*, ***120***,
1119 257-274.

1120 Steiner, M. & Reitner, J. 2001. Evidence of organic structures in Ediacara-type fossils and associated
1121 microbial mats. *Geology, **29**,* 1119–1122.

1122 Stewart, A.D. 1962. On the Torridonian sediments of Colonsay and their relationship to the main
1123 outcrop in north-west Scotland. *Geological Journal*, ***3***, 121-156.

1124 Stewart, A.D. 1963. On certain slump structures in the Torridonian sandstones of Applecross.
1125 *Geological Magazine*, ***100***, 205-218.

1126 Stewart, A.D. 1966. An unconformity in the Torridonian. *Geological Magazine*, ***103***, 462-465.

1127 Stewart, A.D. 1969. Torridonian rocks of Scotland reviewed. *North Atlantic geology and continental*
1128 *drift*, ***12***, 595-608.

1129 Stewart, A.D. 1972. Pre-Cambrian landscapes in Northwest Scotland. *Geological Journal*, ***8***, 111-124.

1130 Stewart, A.D. 1982. Late Proterozoic rifting in NW Scotland: the genesis of the 'Torridonian'. *Journal*
1131 *of the Geological Society*, ***139***, 413-420.

1132 Stewart, A.D., 1988. The Sleat and Torridon Groups. In Later Proterozoic stratigraphy of the northern
1133 Atlantic regions (pp. 104-112). Springer, Boston, MA.

1134 Stewart, A.D. 1991. Geochemistry, provenance and palaeoclimate of the Sleat and Torridon groups in
1135 Skye. *Scottish Journal of Geology*, ***27***, 81–95.

1136 Stewart, A.D. 2002. The later Proterozoic Torridonian rocks of Scotland: their sedimentology,
1137 geochemistry and origin. Geological Society Memoir, 24. Geological Society of London.

1138 Stewart, A.D. & Donnellan, N.C.B. 1992. Geochemistry and provenance of red sandstones in the Upper
1139 Proterozoic Torridon Group in Scotland. *Scottish Journal of Geology*, ***28***, 143-153.

1140 Stewart, A.D. & Irving, E. 1974. Palaeomagnetism of Precambrian sedimentary rocks from NW
1141 Scotland and the apparent polar wandering path of Laurentia. *Geophysical Journal International*, ***37***,
1142 51-72.

1143 Stewart, A.D. & Parker, A. 1979. Palaeosalinity and environmental interpretation of red beds from the
1144 late Precambrian ('Torridonian') of Scotland. *Sedimentary Geology*, ***22***, 229-241.

1145 Straub, K.M. & Wang, Y. 2013. Influence of water and sediment supply on the long-term evolution of
1146 alluvial fans and deltas: Statistical characterization of basin-filling sedimentation patterns. *Journal of*
1147 *Geophysical Research: Earth Surface,* ***118***, 1602-1616.

1148 Strick, R.J., Ashworth, P.J., Sambrook Smith, G.H., Nicholas, A.P., Best, J.L., Lane, S.N., Parsons, D.R.,
1149 Simpson, C.J., Unsworth, C.A. and Dale, J., 2018. Quantification of bedform dynamics and bedload
1150 sediment flux in sandy braided rivers from airborne and satellite imagery. *Earth Surface Processes*
1151 *and Landforms*.

1152 Strother, P.K., Battison, L., Brasier, M.D. &Wellman, C.H. 2011. Earth's earliest non-marine eukaryotes.
1153 *Nature,* ***473***, 505–509.

1154 Strother, P.K. & Wellman, C.H. 2016. Palaeoecology of a billion-year-old nonmarine cyanobacterium
1155 from the Torridon Group and Nonesuch Formation. *Palaeontology,* ***59****,* 89–108.

1156 Van Dijk, W.M., Teske, R., Van de Lageweg, W.I. and Kleinhans, M.G., 2013. Effects of vegetation
1157 distribution on experimental river channel dynamics. *Water Resources Research*, *49*(11), pp.7558-
1158 7574.

1159 Teall, J.J.H. 1907. *The Petrography of the Torridonian Formation. Memoirs of the Geological Survey of*
1160 *Great Britain,* 278–290.

1161 Tirsgaard, H. & Øxnevad, I.E. 1998. Preservation of pre-vegetational mixed fluvio–aeolian deposits in
1162 a humid climatic setting: an example from the Middle Proterozoic Eriksfjord Formation, Southwest
1163 Greenland. *Sedimentary Geology*, ***120***, 295-317.

1164 Todd, S.P. & Went, D.J. 1991. Lateral migration of sand-bed rivers: examples from the Devonian
1165 Glashabeg Formation, SW Ireland and the Cambrian Alderney Sandstone Formation, Channel Islands.
1166 *Sedimentology*, ***38***, 997-1020.

1167 Tooth, S., 2000. Process, form and change in dryland rivers: a review of recent research. *Earth-Science*
1168 *Reviews,* ***51***, 67-107.

1169 Trewin, N.H. 1993. Controls on fluvial deposition in mixed fluvial and aeolian facies within the
1170 Tumblagooda Sandstone (Late Silurian) of Western Australia. *Sedimentary Geology*, ***85***, 387-400.

1171 Tunbridge, I.P. 1984. Facies model for a sandy ephemeral stream and clay playa complex; the Middle
1172 Devonian Trentishoe Formation of North Devon, UK. *Sedimentology,* ***31***, 697-715.

1173 Vogt, T., 1941. Geology of a Middle Devonian cannel coal from Spitsbergen. *Norsk Geologisk Tidsskrift,*
1174 ***21***, 1-12.

1175 Wacey, D., Saunders, M., Roberts, M., Menon, S., Green, L., Kong, C., Culwick, T., Strother, P. and Brasier,
1176 M.D., 2014. Enhanced cellular preservation by clay minerals in 1 billion-year-old lakes. *Scientific*
1177 *reports*, *4*, p.5841.

Walker, R.G. 1976. Facies and facies models, general introduction. *In*: Walker, R.G. (ed). *Facies Models. Geoscience Canada Reprint Series*, ***3***, 21-24.

Wang, Y., Straub, K.M. & Hajek, E.A. 2011. Scale-dependent compensational stacking: an estimate of autogenic time scales in channelized sedimentary deposits. *Geology, **39***, 811-814.

Wellman, C.H. and Strother, P.K., 2015. The terrestrial biota prior to the origin of land plants (embryophytes): a review of the evidence. *Palaeontology*, *58*(4), pp.601-627.

Weissmann, G.S., Hartley, A.J., Scuderi, L.A., Nichols, G.J., Owen, A., Wright, S., Felicia, A.L., Holland, F. and Anaya, F.M.L., 2015. Fluvial geomorphic elements in modern sedimentary basins and their potential preservation in the rock record: a review. *Geomorphology, 250*, pp.187-219.

Went, D.J., 2017. Alluvial fan, braided river and shallow-marine turbidity current deposits in the Port Lazo and Roche Jagu formations, Northern Brittany: relationships to andesite emplacements and implications for age of the Plourivo-Plouézec Group. Geological Magazine, 154(5), pp.1037-1060.

Went, D.J. and McMahon, W.J., 2018. Fluvial products and processes before the evolution of land plants: Evidence from the lower Cambrian Series Rouge, English Channel region. *Sedimentology*, *65*(7), pp.2559-2594.

Williams, G.E. 1966. Palaeogeography of the Torridonian Applecross group. *Nature*, ***209***, 1303-1306.

Williams, G.E. 2001. Neoproterozoic (Torridonian) alluvial fan succession, northwest Scotland, and its tectonic setting and provenance. *Geological Magazine, **138***, 161–184.

Williams, G.E. & Foden, J. 2011. A unifying model for the Torridon Group (early Neoproterozoic), NW Scotland: Product of post-Grenvillian extensional collapse. *Earth-Science Reviews, **108***, 34–49.

Wohl, E., 2013. Floodplains and wood. *Earth-Science Reviews, **123,*** 94-212.

1199 Wolman, M.G. & Brush, L.M., 1961. *Factors controlling the size and shape of stream channels in coarse*
1200 *noncohesive sands*. US Government Printing Office.

1201 Xu, J. 2002. River sedimentation and channel adjustment of the lower Yellow River as influenced by
1202 low discharges and seasonal channel dry-ups. *Geomorphology*, ***43***, 151-164.

1203 Zhang, Z. 1982. Upper Proterozoic microfossils from the Summer Isles, NW Scotland. Palaeontology,
1204 25, 443–460.

1205 Zhang, Z., Diver, W. & Grant, P.R. 1981. Microfossils from the Aultbea Formation, Torridon Group, on
1206 Tanera Beg, Summer Isles. Scottish Journal of Geology, 17, 149–154,
1207 https://doi.org/10.1144/sjg17020149

1208 **Figure Captions**

1209 **Figure 1.** Geographic and stratigraphic setting. Left and top right: Geological map of the Torridonian
1210 outcrop belt (modified after Stewart, 2002). Numbers mark study locations listed in Table 1. Bottom
1211 right: Stratigraphic relationships between the constituent unit of the Torridonian Sandstones. Total
1212 Torridonian Sandstone stratigraphic thickness is approximately 11 km.

1213 **Figure 2.** Examples of erosionally-based cross-stratified sheets: A) Prominent basal erosional
1214 surface (Loc. 22. Liathach); B) Liathach SW facing flank (depositional-dip section); C) Sandstone
1215 dominated deposit (Loc. 12. Stac Pollaidh). Bag is 37 centimetres high; D) Gravel dominated deposit
1216 (Loc. 5. Assynt). Person is 187 centimetres tall. St/Gt = Trough cross-stratified sandstone/granular
1217 sandstone; Sp = Planar cross-stratified sandstone. Red arrowheads indicate average palaeocurrent
1218 direction.

1219 **Figure 3.** Sedimentological features of erosionally based cross-stratified sheet deposits: A) Pebbly
1220 sandstone (Loc. 3. Handa Island). Notebook is 13 cm wide; B) Trough cross-stratified medium-
1221 grained sandstone (Loc. 4. Quinag). Hammer head is 18 cm wide; C) Granule to pebble lag flooring a

lower erosional boundary (Loc. 6. Stoer); D) Intraformational mud clasts flooring a lower erosional boundary (Loc. 22. Liathach). Pen is 14 cm long; E) Trough cross-stratification (Loc. 3. Handa Island); F) Planar cross-stratification (Loc. 3. Handa Island).

Figure 4. Examples of soft-sediment deformation in Torridon alluvium. A) Small-scale contortions within a single bedded deposit (Loc. 27. Toscaig). Coin (circled) is 2 cm wide; B) Soft-sediment deformed horizons displaying predominant vertical shear (Loc. 22. Liathach); C) Chaotically disturbed stratification (Loc. 17. Aultbea). Notebook is 21 cm long; D) Laterally persistent soft-sediment deformed horizon displaying significant vertical shear (Loc. 22. Liathach). Circled in Figure 4.2B; E) Laterally persistent, top-truncated soft-sediment deformed horizon (Loc. 27. Toscaig). Metre rule for scale; F) Line drawing of E.

Figure 5. Preserved depositional topography. A) Wide trough cross-stratified sets and soft-sediment deformation; B) Soft-sediment deformed trough-cross stratification; C) 2-metre-wide trough-cross stratified set. All Bealach na Bà (Loc. 26). Bag is 35 cm high.

Figure 6. Stratigraphic relationships between inclined accretionary strata and channel-bedform deposits: A) A channel-bedform deposit (1) is overlain by multiple large sets of inclined planar accretionary strata (2) accreting at a high angle to local palaeoflow. Each inclined set abuts against a common underlying surface (3). Soft-sediment deformation is observed in inclined accretionary strata (4) (Loc. 22. Liathach); B) An erosion surface (1) marks the base of the channel-bedform deposit (2). Overlying inclined accretionary strata (3) are accreting into the outcrop at a high angle to local palaeoflow (Loc. 23.Seana Mheallan); C) A multistorey channel-bedform sequence (1) is overlain by inclined planar accretionary strata (2). Inclined accretionary strata accrete in approximately the same orientation as local palaeoflow (3). An erosion surface marks the base of an overlying channel-bedform deposit (4) (Loc. 22. Liathach). Blue lines in schematic sketches mark accretion surfaces. I.A.S = Inclined accretionary strata. St = Trough cross-stratified sandstone; Sp =

Planar cross-stratified sandstone; SS = Soft-sediment deformation. Red arrowheads indicate average palaeoflow direction. Blue arrowheads indicate average accretion orientation.

Figure 7. Sedimentological characteristics of inclined accretionary strata. Channel-bedform deposit (1) overlain by sigmoidal inclined accretionary strata (2) accreting nearly perpendicular to local palaeoflow (Loc. 24. Upper Loch Torridon). Red arrowhead indicates average palaeoflow. Blue arrowhead indicates average accretion orientation. Bag is 35 centimetres high; B) Large sigmoidal inclined accretionary strata. Metre rule for scale (Loc. 22. Liathach); C) Low-angle accretionary strata (2) overlying trough cross-stratified channel-bedform deposit (2) (Loc. 23. Seana Mheallan). Bag is 35 centimetres high; D) Oversteepened sigmoidal inclined accretionary strata (Loc. 22. Liathach); E) Large-scale sigmoidal and low-angle accretionary strata showing significant soft-sediment deformation (Loc. 20. Diabaig); F) Horizontal-stratification occurring in outcrop directly above large-scale inclined planar accretionary strata (not shown in figure) (Loc. 22. Liathach). Bag is 35 centimetres high. St = Trough cross-stratified sandstone; Sl = Low-angle cross-stratified sandstone; Sh = Horizontally-stratified sandstone.

Figure 8. Examples of inclined accretionary strata erosively overlain by channel-bedform deposits. A) Alligin (Loc. 21). Metre rule for scale. Red arrows highlight boundary between inclined accretionary strata and channel-bedform deposit; B) Roadside outcrop near Stac Pollaidh (Loc. 12). Sigmoidal sets accreting near perpendicular to local flow direction (125°). I.A.S = Inclined accretionary strata

Figure 9. Discontinuous mudstone to very fine-grained sandstone deposits: A) Channel abandonment deposits, composed of plane-parallel laminated mudstone and siltstone (Loc. 6. Stoer Peninsula). Metre rule for scale; B) Discontinuous siltstone bed erosively overlain by a channel-bedform deposit (Loc. 22. Liathach). Bag is 35 cm high; C) Thick mudstone deposit erosively overlain by a channel-bedform deposit (Loc. 13. Tanera Beg). Metre rule for scale; D) Preserved

intraformational mud clasts (Loc. 11. Achiltibuie). Metre rule for scale; E) Ripple cross- and parallel-laminated deposits showing incipient soft-sediment deformation (Loc. 19. North Erradale). Pen for scale is 2 cm long; F) Ripple cross-laminated very fine sandstone deposit (Loc. 12. Stac Pollaidh). Compass for scale is 11 cm long.

Figure 10. Schematic diagram illustrating the relationship between the defined architectural deposits. t = thickness. Width constraints: channel-bedform deposits, >100 metres in both depositional-dip and depositional-strike sections; barform deposits, > 100 metres in depositional-dip sections and up to 70 metres in depositional strike sections (constrained by available exposure); out-of-channel deposits, up to 30 metres in both depositional-dip and strike sections.

Figure 11. Multistorey channel-bedform sequence exposed in three-dimensions (Loc. 22. Liathach). Sequence comprises of 4 channel-bedform deposits (labelled 1 to 4), each separated by an erosional boundary.

Figure 12. Example channel-belts. A multistorey channel-bedform sequence (1,2,3) overlain by a genetically related barform deposit (4) accreting at a similar angle to local palaeoflow comprise the lowest channel-belt. An erosion surface (5) overlain by a channel-bedform deposit (6) and a genetically related barform deposit (7) accreting at a low angle to local palaeoflow comprise the middle channel-belt. Channel-bar thickness can in this instance be used as a proxy for minimum flow depth Section (5.6.2). An erosion surface (8) overlain by a thick channel-bedform deposit (9) marks the lowest potion of the uppermost channel belt (genetically related barform deposits out of shot). Liathach (Loc. 22). Asterisk marks a possible remnant bar deposit preserved within a channel-bedform deposit.

Figure 13. Example channel-belt sequence (Loc. 23. Seana Mheallan). A multistorey channel-bedform sequence is overlain by a barform deposit. Red arrowhead indicates average palaeocurrent direction of three figured channel-bedform deposits. Blue arrowhead indicates accretion direction of

figured barform deposit. Further examples of superbly preserved channel-bar sequences can be found in Owen and Santos (2014; their figure 8).

Figure 14. Example composite barform sequence (Loc. 22. Liathach). Succession consists of three stacked barform deposits (labelled 1 to 3) each separated by a planar erosional surface. Metre rule for scale.

Figure 15. Details of Seana Mheallan section. A) Location map. Centre of image approximately 57°32'45''N; 5°30'48''W. See Figure 1 and Table 1 for location within outcrop belt; B) Seana Mheallan. Dashed line indicates logged section; C) Out-of-channel material (arrowed) erosively overlain by a channel-bedform deposit (1) overlain by a genetically related downstream-accreting barform deposit (B). Bag is 37 cm high; D) Channel-bedform deposit (1) overlain by genetically related downstream-accreting barform deposit (2). Bag is 37 cm high; E) Logged section of Torridon alluvium exposed at Seana Mheallan. Abbreviations: ms=medium-grained sand; cs = coarse-grained sand; gr = gravel. Palaeoflow and accretion directions presented as average for each deposit (min n=2; max n=13).

Figure 16. Map of palaeoflow and barform accretion directions measured across the Torridon outcrop belt. Torridon alluvium highlighted in grey. Values attached to each rose diagram represent the total number of readings.

Figure 17. Photomosaic of Torridon alluvium cliff face at Cape Wrath (Loc. 1) (see Figure 1 and Table 1 for precise location). Cliff face is orientated marginally oblique to regional palaeoflow (inaccessibility of largely sheer cliff face meant palaeoflow orientations could not be directly recorded). The photomosaic demonstrates the dominant tabular architecture which typifies Torridon alluvium and is archetypal for many global pre-vegetation alluvial successions.

Figure 18. Example reticulate marks in the Diabaig Formation. A-D) Diabaig (Loc. 20); E) Raasay (Loc. 28); F) Achiltibuie (Loc. 11). Compass-clinometre in (A) is 9 cm long. Pen lid in (B) is 3 cm long. Coin in (F) has a diameter of 2.5 cm.

Figure 19. Examples of sedimentary surface textures with possible microbial origin in the Diabaig Formation. A) Spindle-shaped cracks (Diabaig [Loc. 20]); B) Wrinkle marks (Diabaig [Loc. 20]); C-D) Circular impressions (C: Diabaig [Loc. 20]; D: Achiltibuie [Loc. 11]); E) 'Arumberia'-like marking (Raasay [Loc. 28]); F) 'Lizard-Skin' texture (Road section connecting Alligin [Loc. 21] and Diabaig [Loc. 20]).

Figure 20. Thin sections showing finely laminated sediment consisting of thin, organic-rich laminae and flakes, alternating with very-fine sandstone and siltstone horizons. (A-B); Laminae displaying brittle deformation indicate cohesive behavior of the organic-rich horizons (A: Upper Loch Torridon [Loc. 24]; B: Seana Mheallan [Loc. 23]); C) Organic laminae displaying distinctive wavy-crinkly morphology here interpreted as an ancient microbial mat horizon (arrowed) (Loc. 22. Liathach); D) Deformed organic laminae stochastically interbedded with clastic grains (Loc. 6. Stoer Peninsula).

Figure 21. Sedimentary surface textures from the Cailleach Head Formation. A) Branching 'spindle-shaped' cracks and 'triple-junction bird's feet; B) Positive-epirelief 'domes'; C) 'Elephant-skin' texture. Coin has diameter of 2.5 cm; D) Manchuriophycus. (A-C) Cailleach Head (Loc. 14); D) Gruinard Island (Loc. 16)

Table captions

Table 1. Geographic coordinates of all field locations utilized in this study. For map locations see Figure 1.

Table 2. Glossary of terms used in this paper.

Table 3. List of architectural elements referred to in this study. After Miall (1985, 1996), Fielding (2006) and Long (2011)

Table 4. Measurements of channel-bedform deposit – barform deposit thickness separated by geographic area. It is not possible to precisely determine stratigraphic position for Torridon alluvium, due to the absence of marker beds, but in general the succession gets increasingly younger southwards.

1358 Figure 1

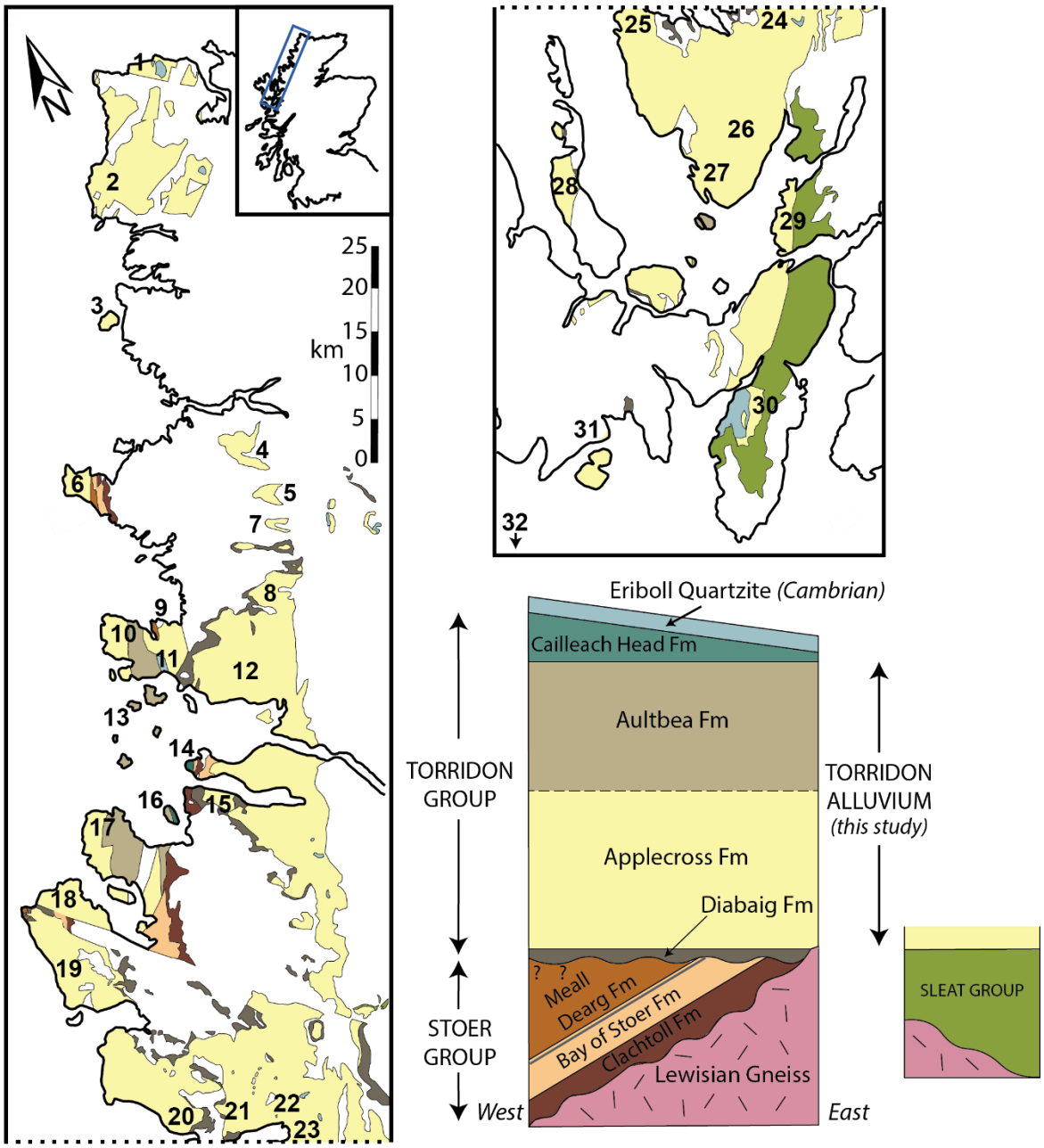

1359

1360

1361

1362 Figure 2

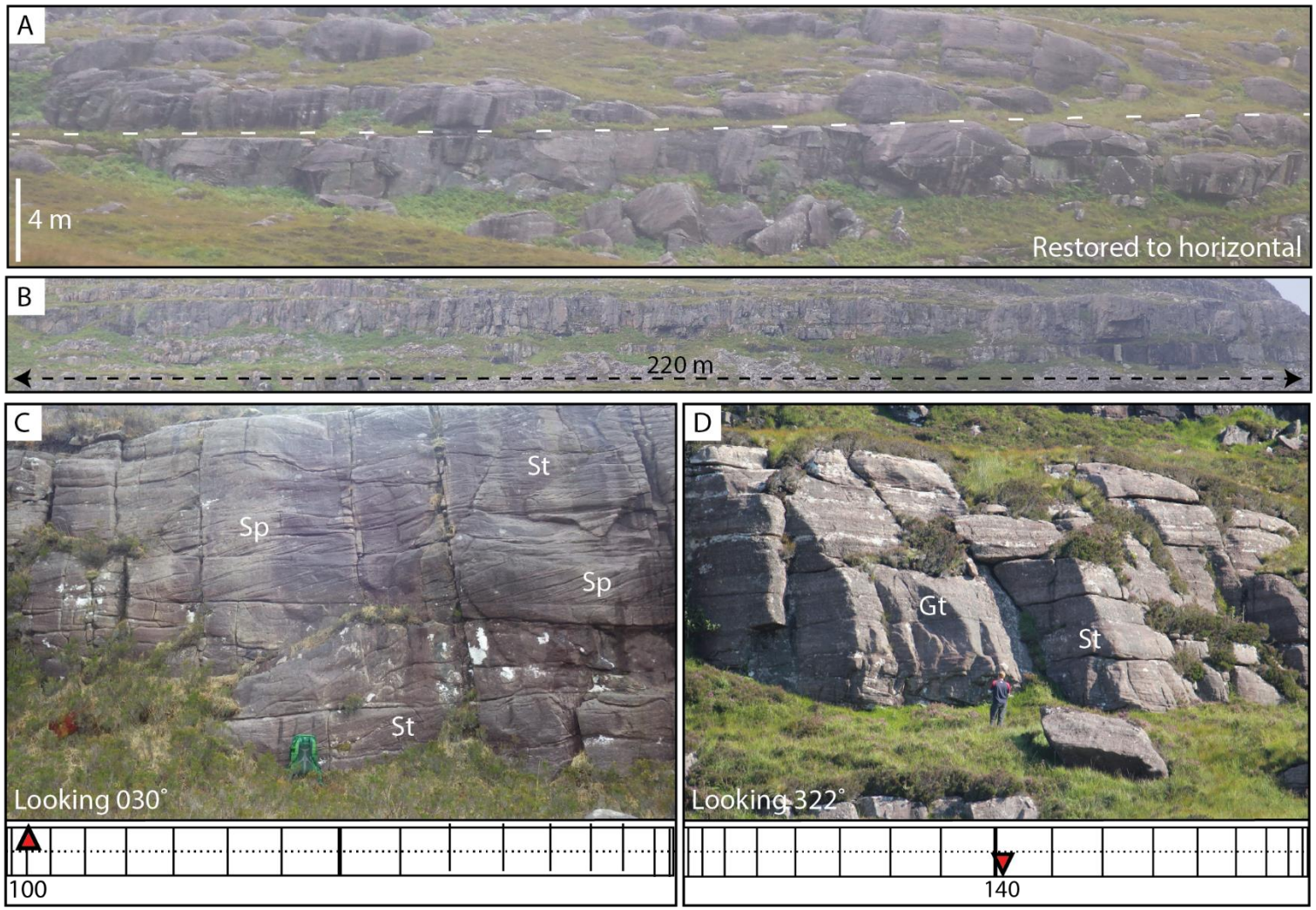

1363

1364 Figure 3

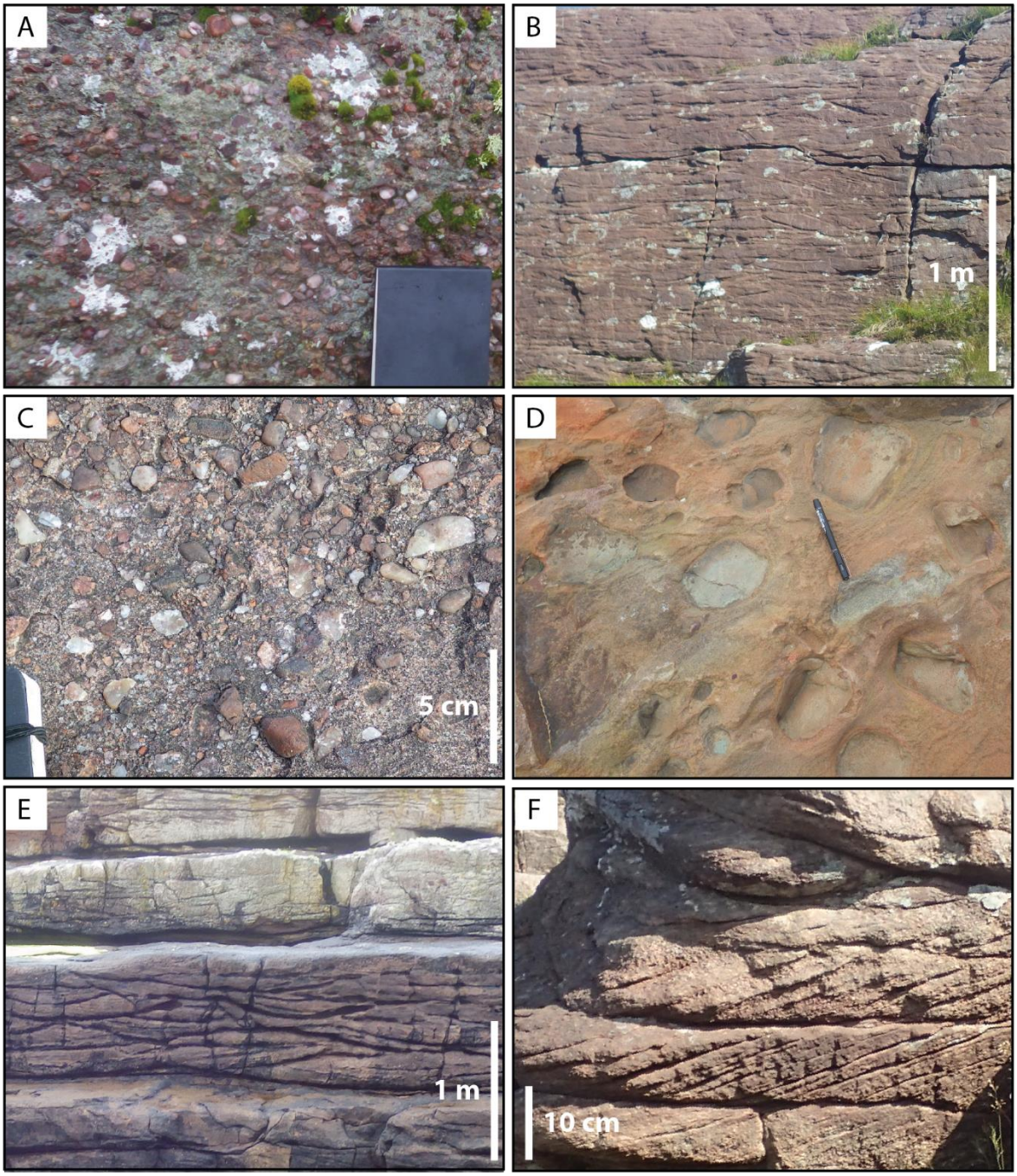

1365

1366

1367

1368 Figure 4

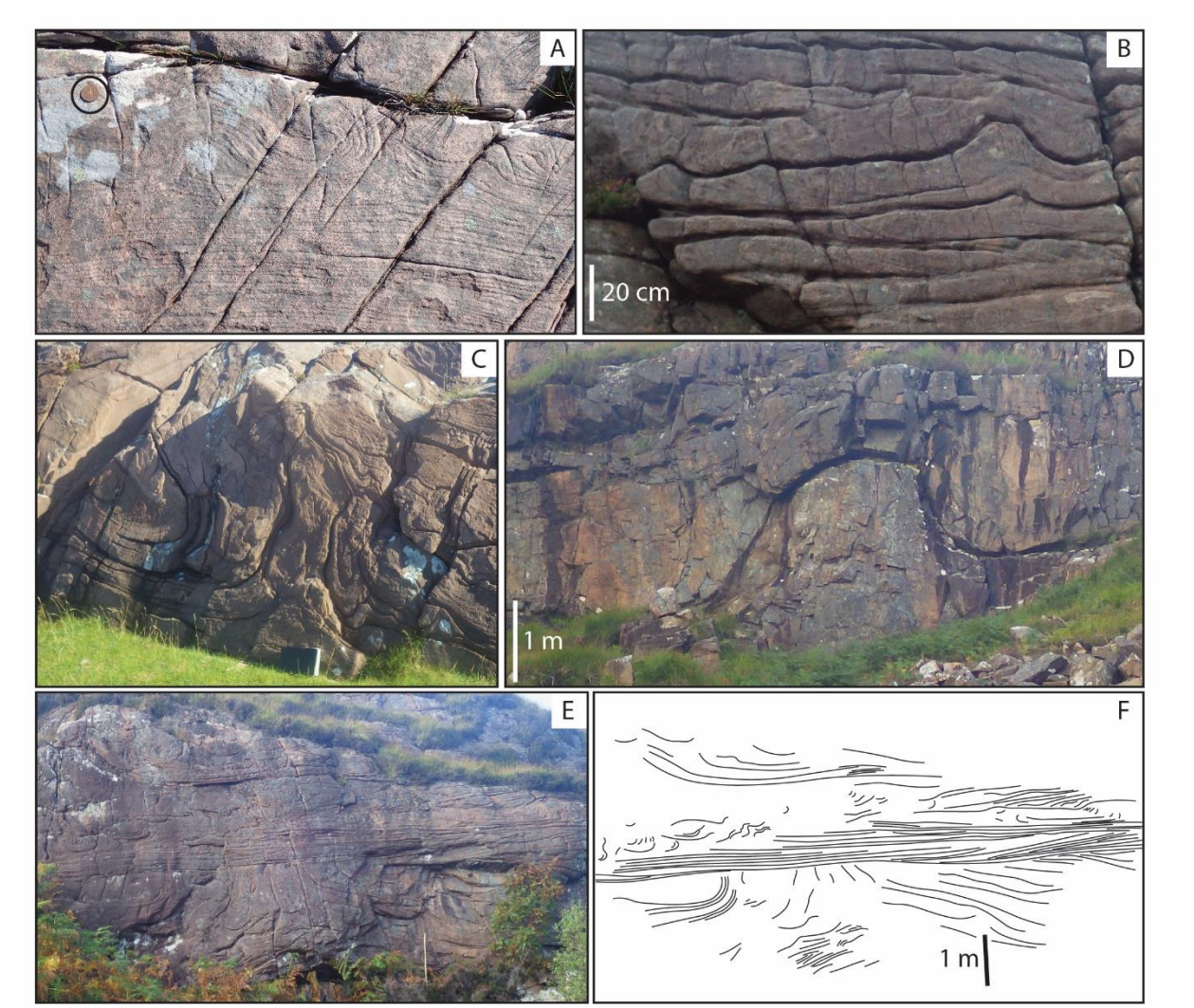

1369

1370

1371

1372

1373

1374

1375

1376 Figure 5

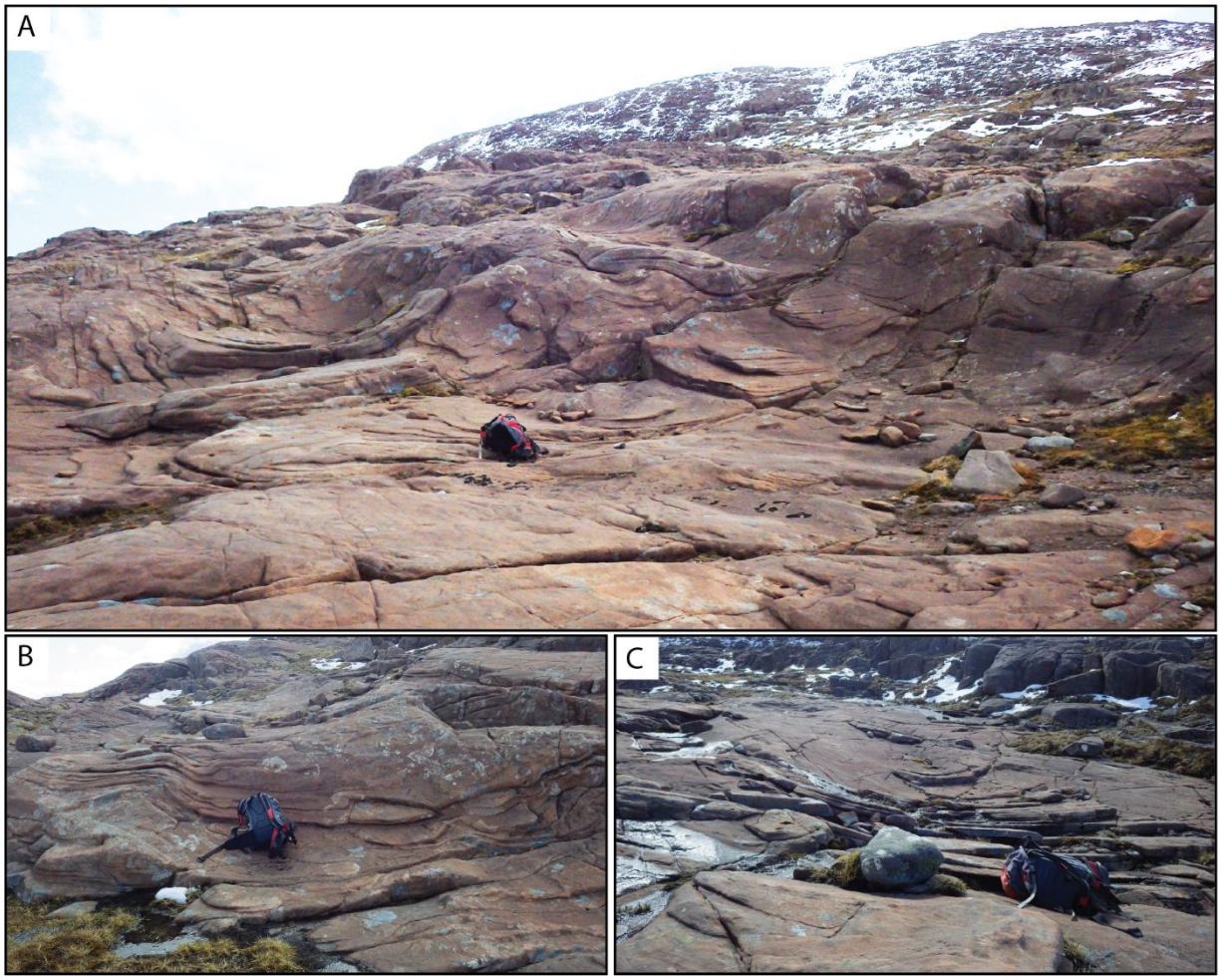

1377

1378

1379

1380

1381

1382

1383

1384 Figure 6

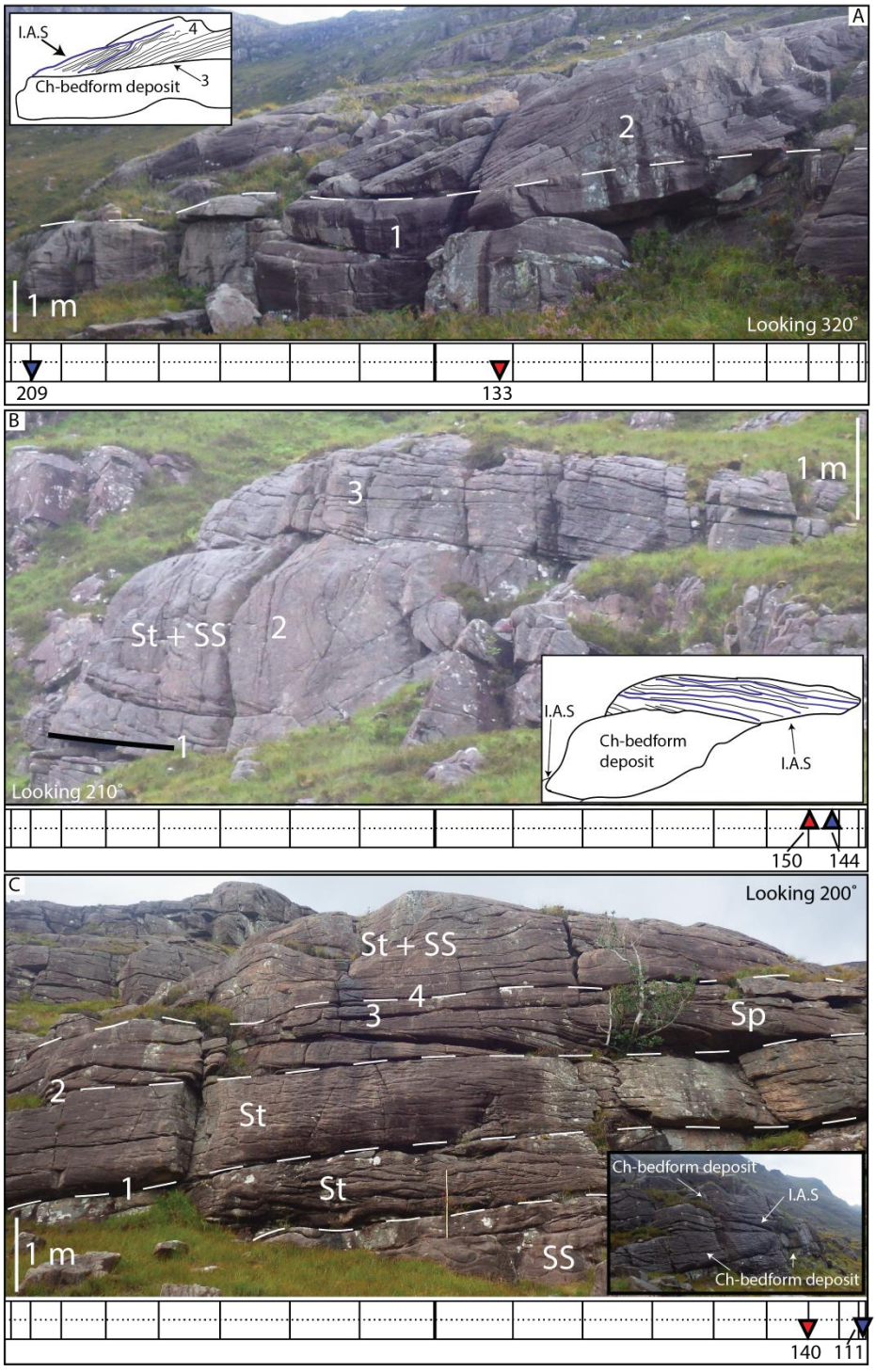

1385

1386

1387 Figure 7

1388

1389

1390

1391

1392

1393

1394 Figure 8

1395

1396

1397

1398

1399

1400

1401

1402

1403

1404 Figure 9

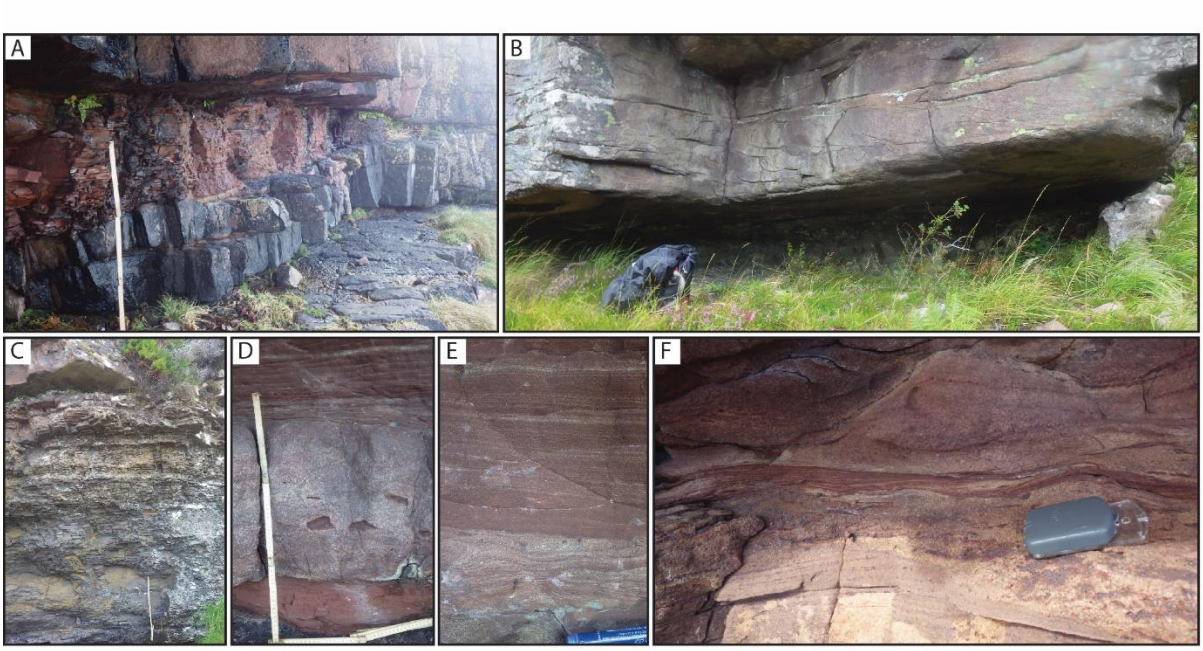

1405

1406

1407

1408

1409

1410

1411

1412

1413

1414

1415

1416 Figure 10

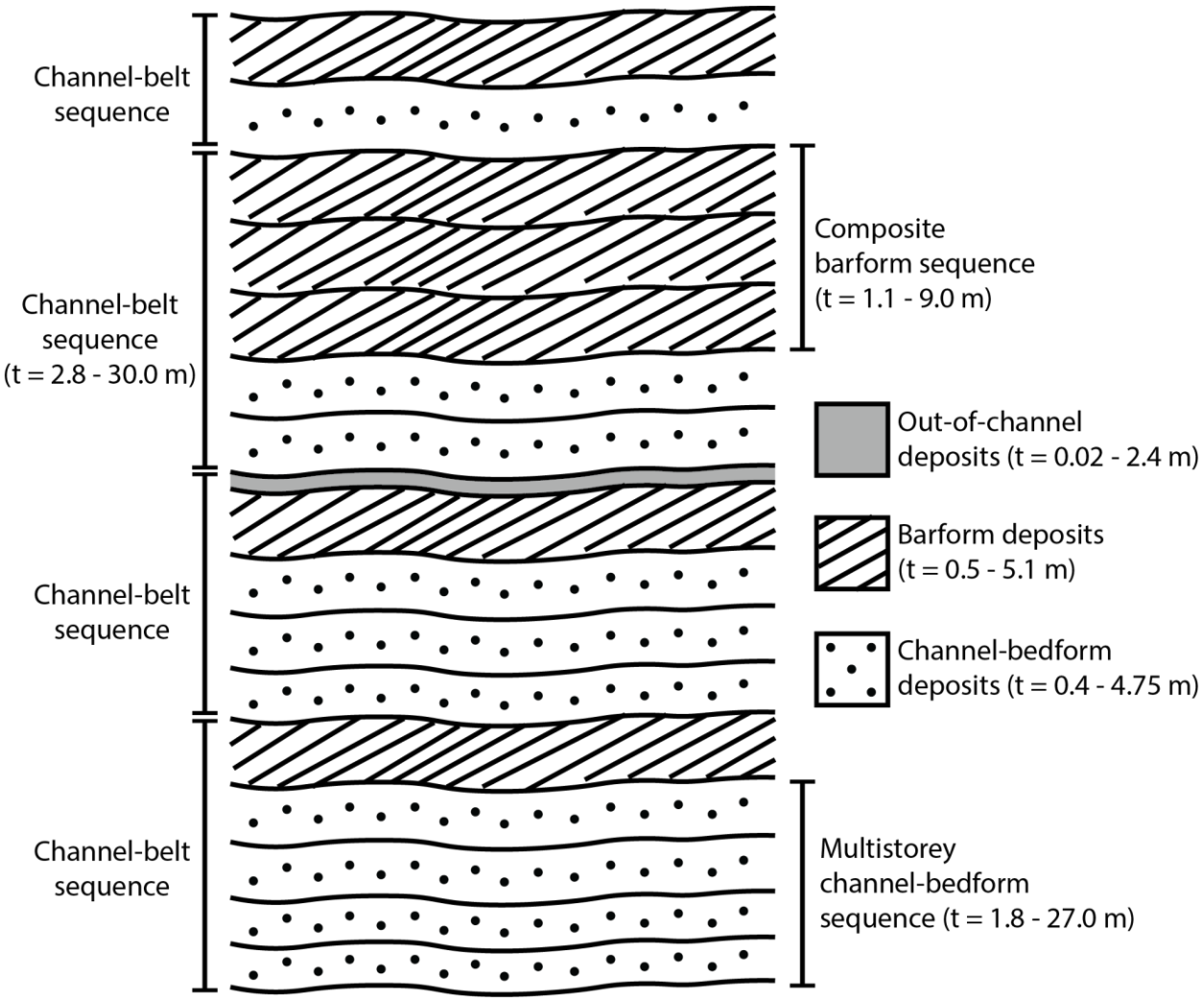

1417

1418

1419

1420

1421

1422

1423

1424 Figure 11

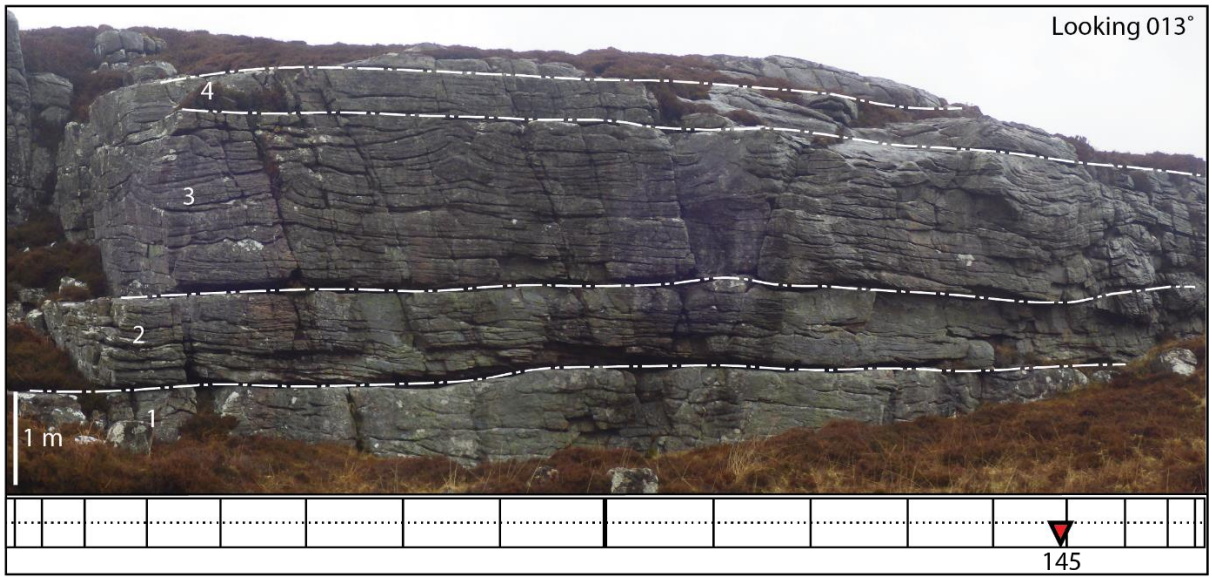

1425

1426

1427

1428

1429

1430

1431

1432

1433

1434

1435

1436

1437 Figure 12

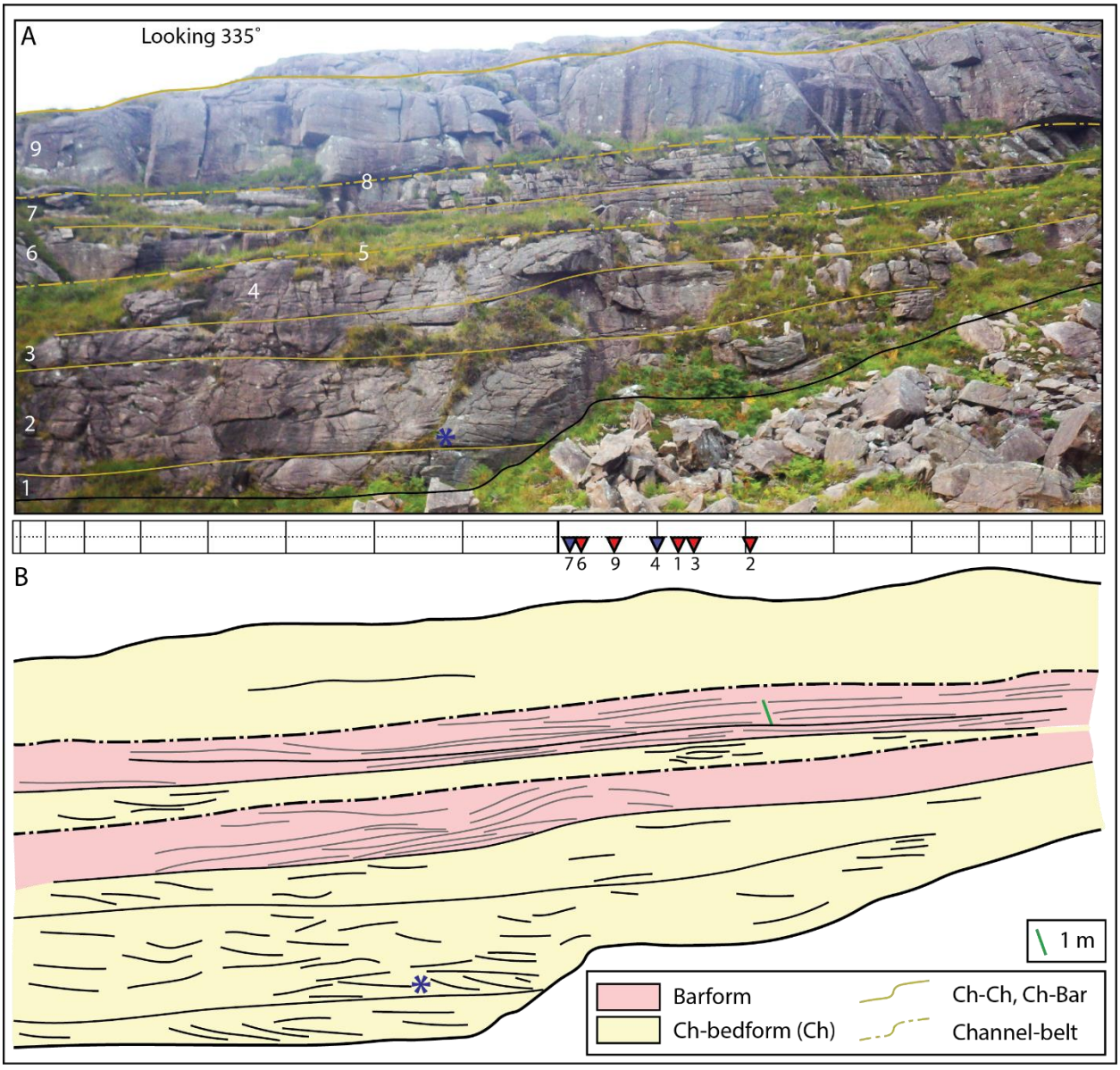

1438

1439

1440

1441

1442

1443 Figure 13

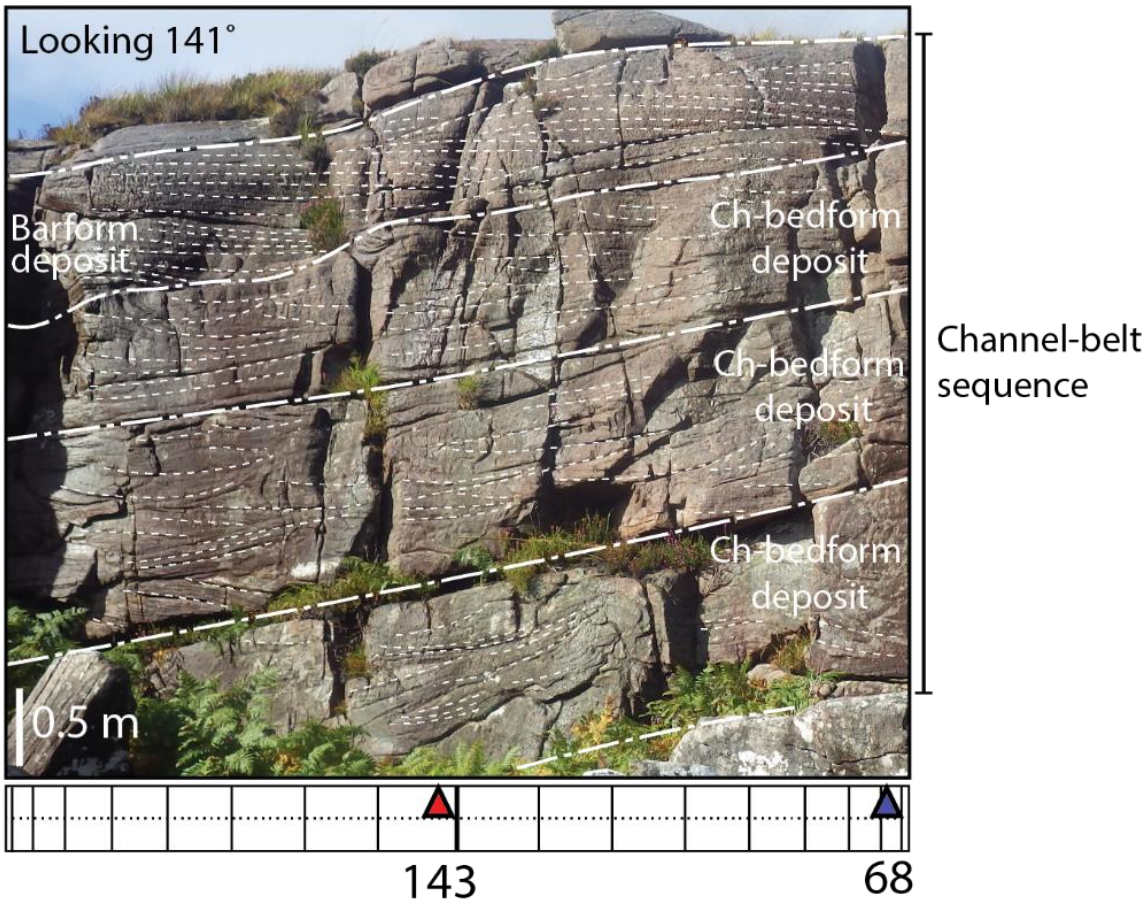

1444

1445

1446

1447

1448

1449

1450

1451

Figure 14

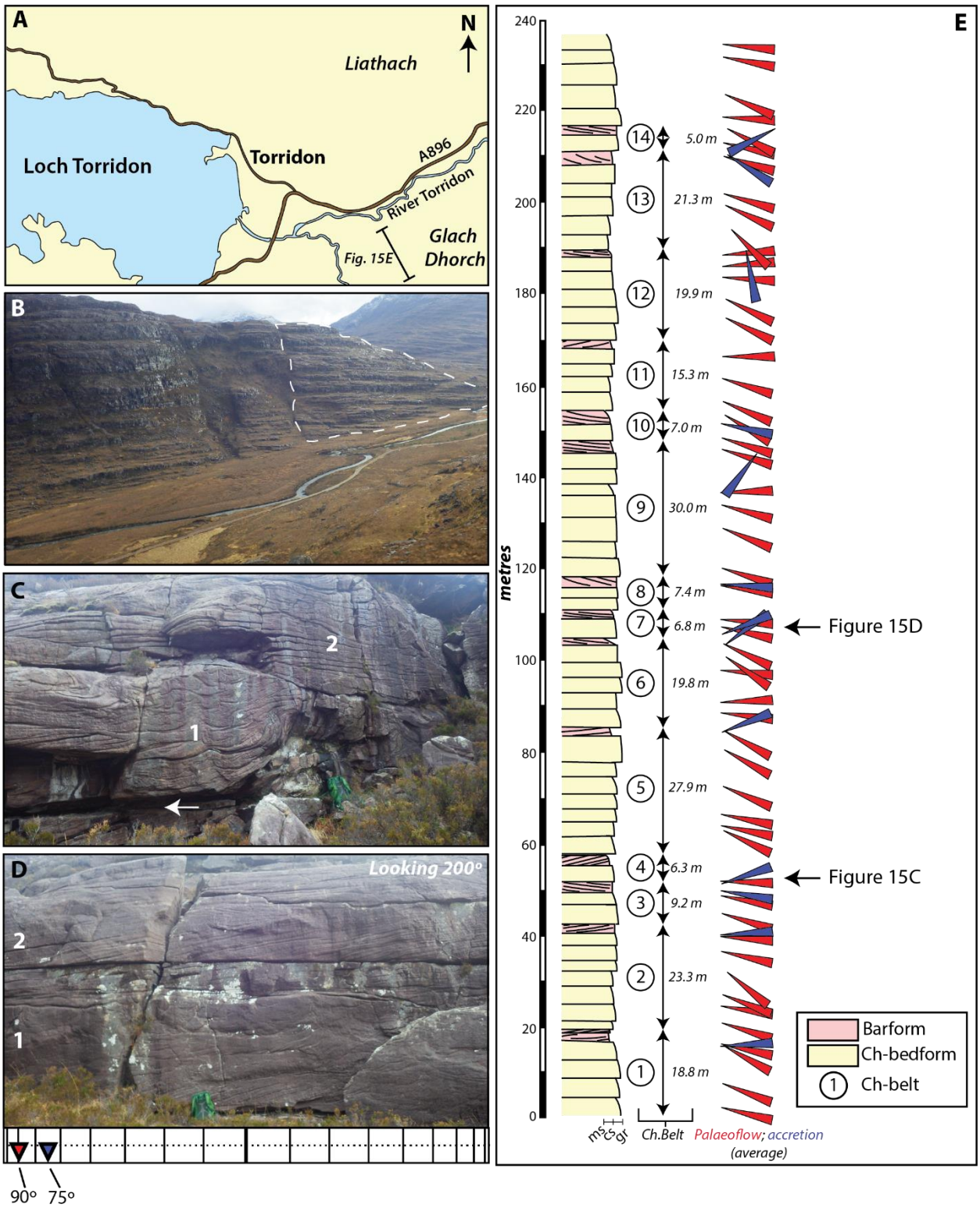
A
N
Liathach
Loch Torridon
Torridon
A896
River Torridon
Glach Dhorch
Fig. 15E
B
C
2
1
D
Looking 200°
2
1
90°
75°
E
metres
240
220
200
180
160
140
120
100
80
60
40
20
0
14
5.0 m
13
21.3 m
12
19.9 m
11
15.3 m
10
7.0 m
9
30.0 m
8
7.4 m
7
6.8 m
6
19.8 m
5
27.9 m
4
6.3 m
3
9.2 m
2
23.3 m
1
18.8 m
Figure 15D
Figure 15C
Barform
Ch-bedform
Ch-belt
ms
gr
Ch.Belt
Palaeoflow; accretion (average)

1463

1464

1465 Figure 16

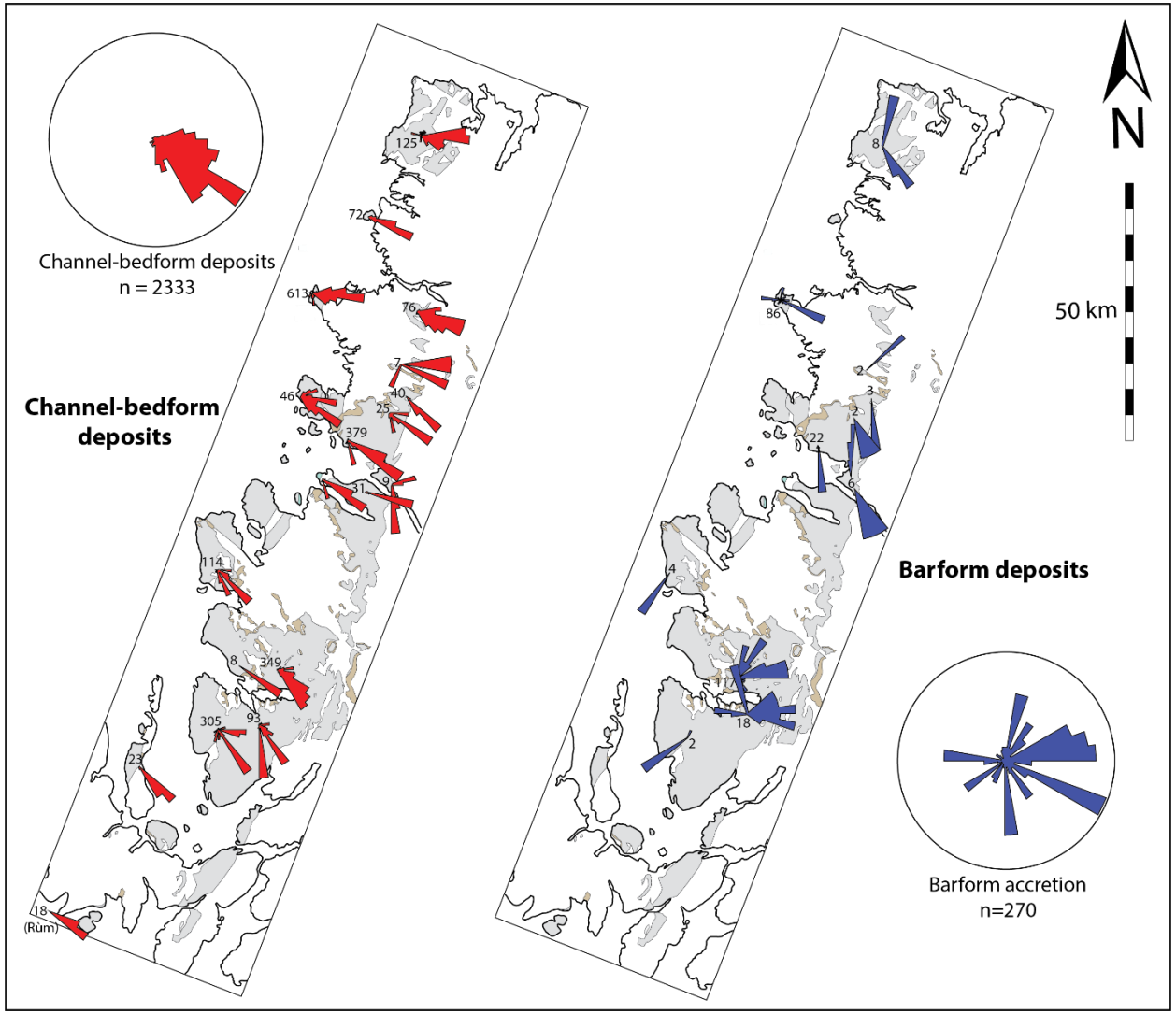

1466

1467 Figure 17

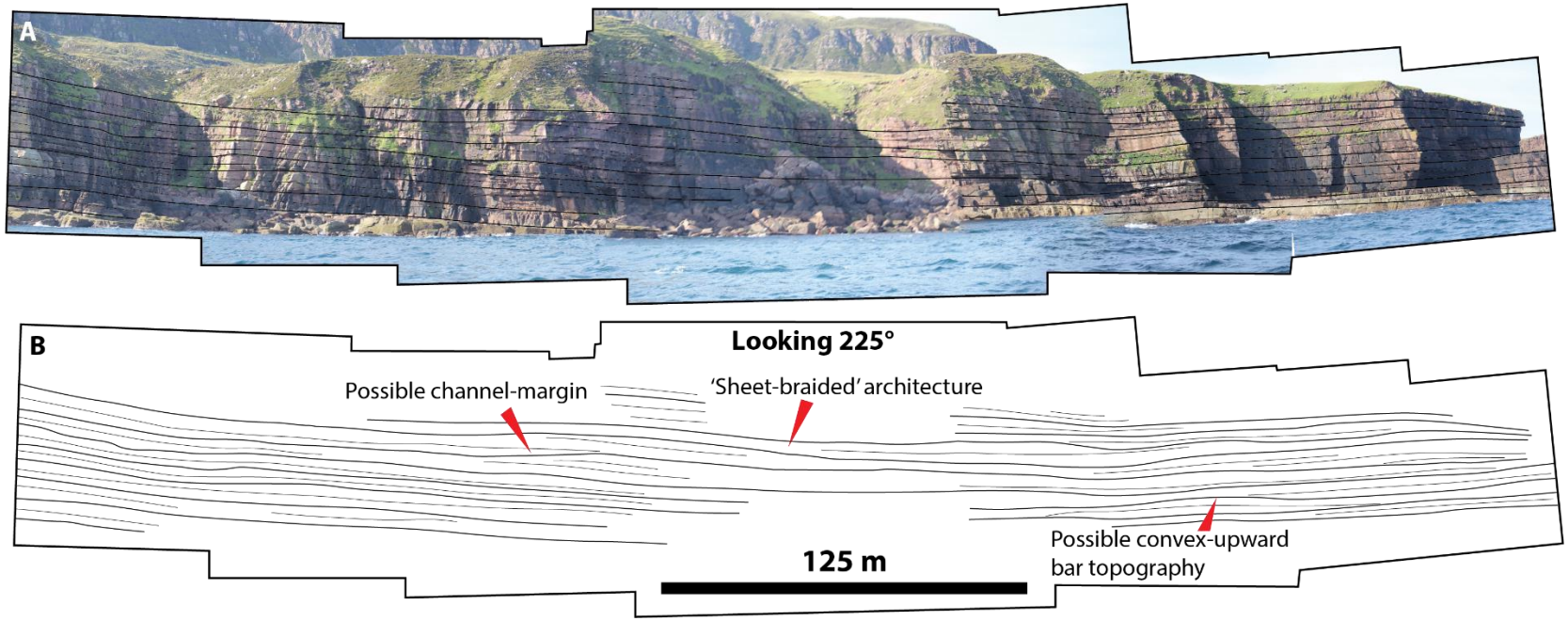

1468

1469

1470

1471

1472

1473 Figure 18

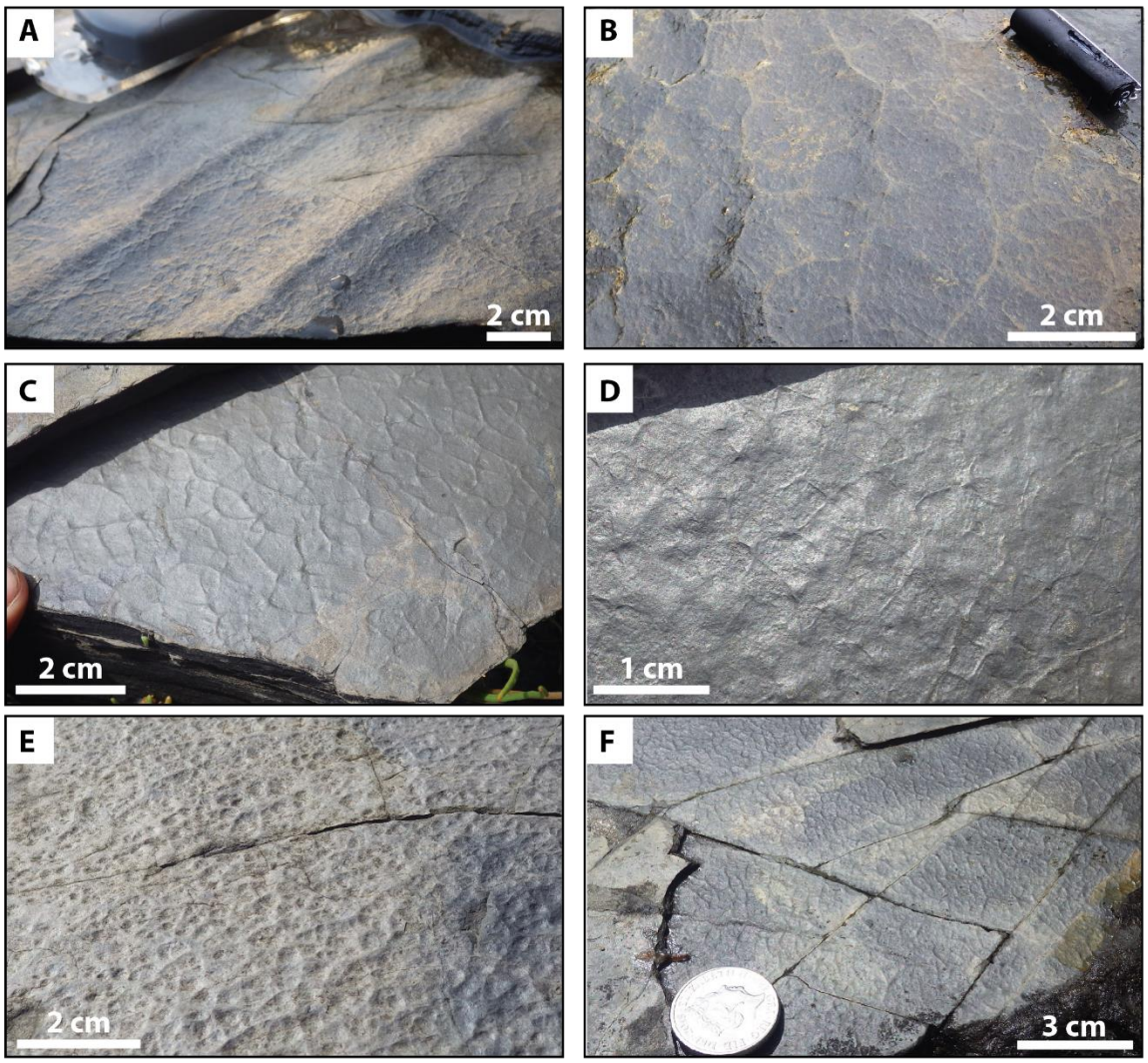

1474

1475

1476

1477

1478

1479

1480 Figure 19

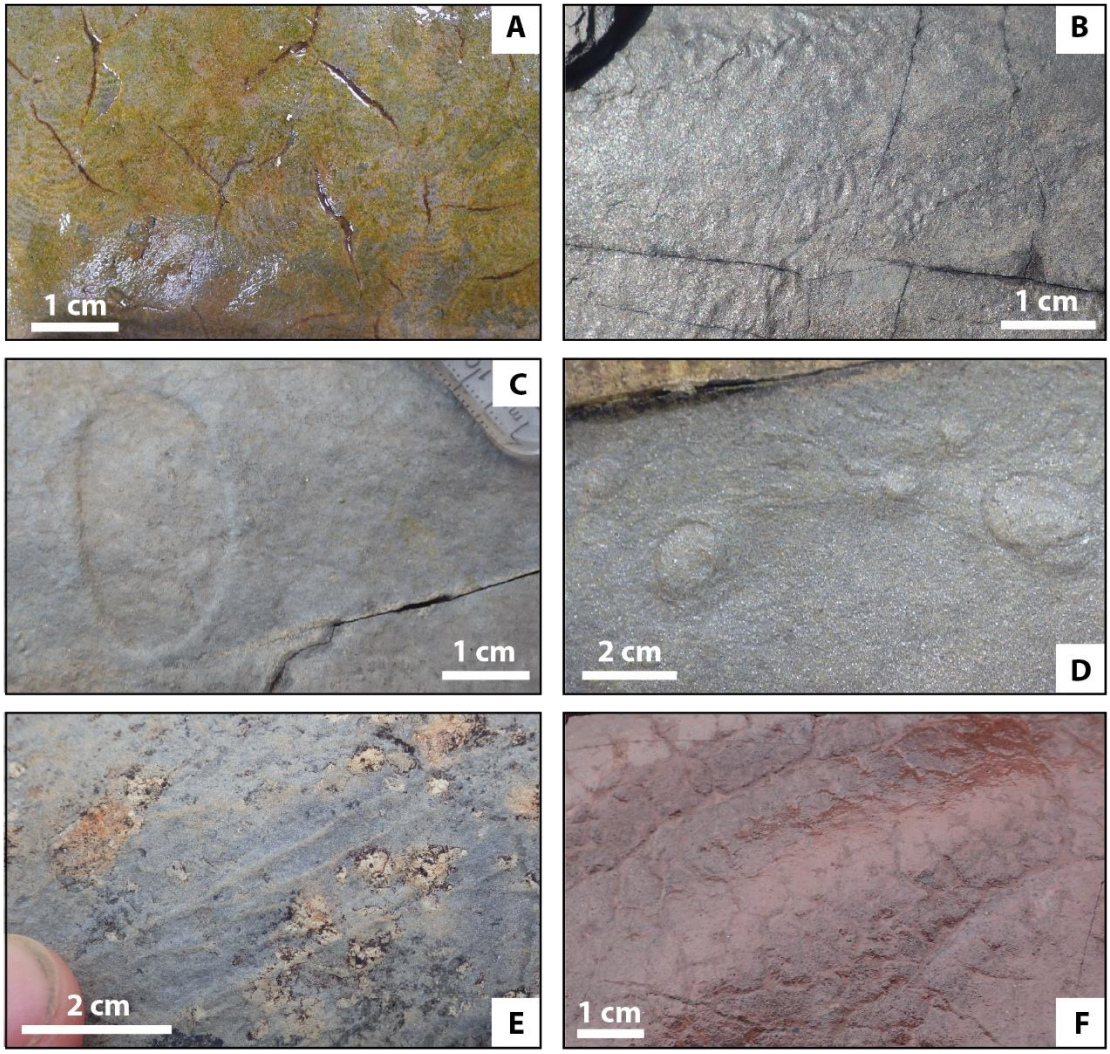

1481

1482

1483

1484

1485

1486

1487 Figure 20

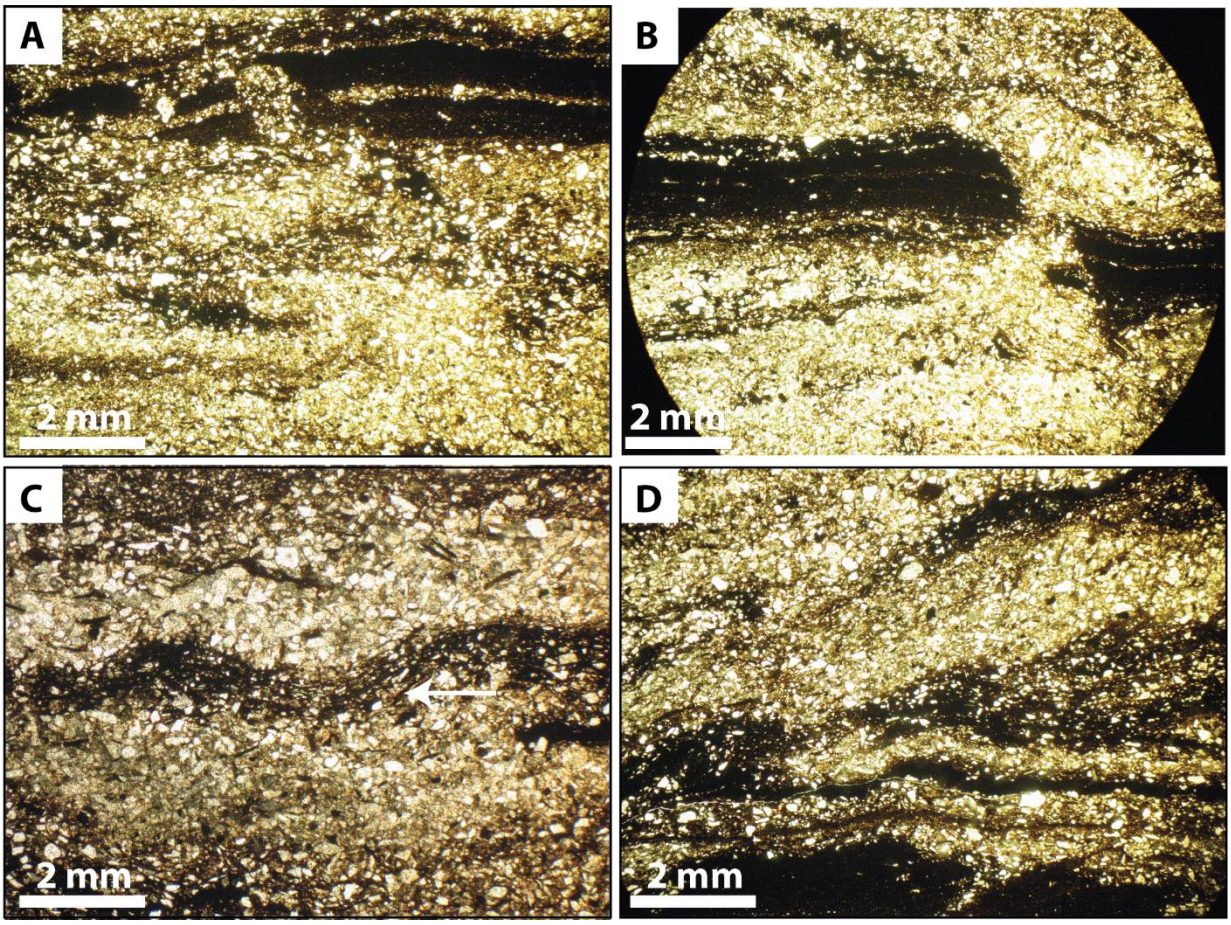

1488

1489

1490

1491

1492

1493

1494

1495

1496 Figure 21

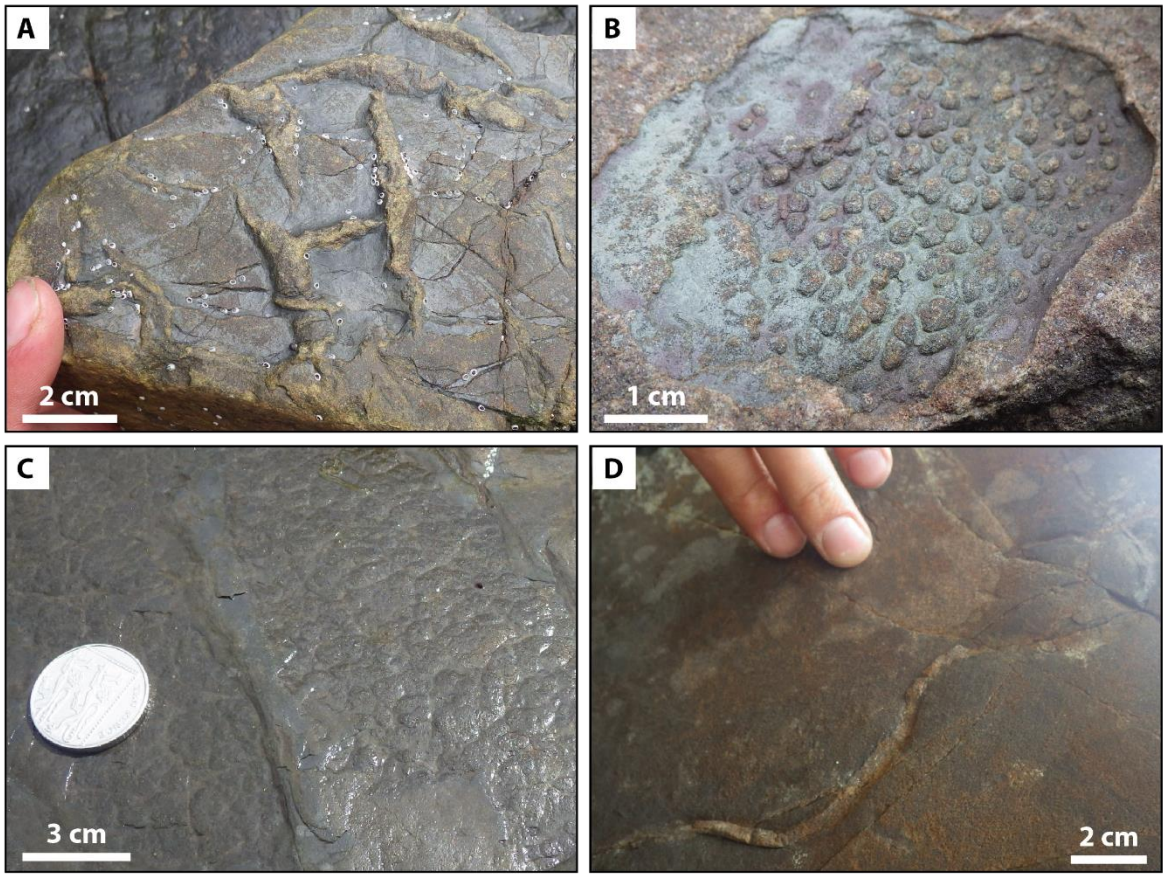

1497

1498

1499

1500

1501

1502

1503

1504

Table 1

Torridon Group locations	
1. Cape Wrath	58° 37’ 33’’N, 4° 59’ 51’’W
2. Sandwood Bay	58° 32’ 14’’N, 5° 03’ 34’’W
3. Handa Island	58° 23’ 02’’N, 5° 11’ 14’’W
4. Quinag	58° 12’ 54’’N, 5° 03’ 00’’W
5. Assynt	58° 10’ 22’’N, 5° 01’ 50’’W
6. Stoer peninsula	58° 12’ 05’’N, 5° 20’ 15’’W
7. Suilven	58° 00’ 11’’N, 5° 07’ 59’’W
8. Inverpolly	58° 03’ 12’’N, 5° 11’ 44’’W
9. Enard Bay	58° 04’ 33’’N, 5° 19’ 12’’W
10. Reiff	58° 04’ 12’’N, 5° 20’ 51’’W
11. Achiltibuie	58° 01’ 81’’N, 5° 21’ 65’’W
12. Stac Pollaidh	58° 02’ 35’’N, 5° 12’ 20’’W
13. Tanera Beg	58° 00’ 26’’N, 5° 27’ 02’’W
14. Cailleach Head	57° 52’ 25’’N, 5° 16’ 62’’W
15. Stattic Point	57° 52’ 11’’N, 5° 20’ 24’’W
16. Gruinard Island	57° 52’ 59’’N, 5° 28’ 20’’W
17. Aultbea	57° 50’ 32’’N, 5° 35’ 11’’W
18. Bac an Leth-choin	57° 50’ 50’’N, 5° 44’ 48’’W
19. North Erradale	57° 45’ 07’’N, 5° 48’ 09’’W
20. Diabaig	57° 34’ 43’’N, 5° 42’ 13’’W
21. Alligin	57° 35’ 25’’N, 5° 34’ 20’’W
22. Liathach	57° 35’ 00’’N, 5° 29’ 00’’W
23. Seana Mheallan	57° 32’ 25’’N, 5° 28’ 18’’W
24. Upper Loch Torridon	57° 31’ 39’’N, 5° 30’ 39’’W
25. Fearnmore	57° 344’ 39’’N, 5° 48’ 56’’W
26. Bealach na Bà	57° 25’ 08’’N, 5° 42’ 32’’W
27. Toscaig	57° 22’ 26’’N, 5° 48’ 49’’W
28. Raasay	57° 26’ 22’’N, 6° 02’ 10’’W
29. Kyle of Lochalsh	57° 16’ 53’’N, 5° 42’ 12’’W
30. Ord	57° 08’ 55’’N, 5° 56’ 26’’W
31. Camasunary	57° 11’ 40’’N, 6° 06’ 54’’W
32. Rùm	57° 01’ 14’’N, 6° 16’ 07’’W

1512 Table 2

TERM	DEFINITION
'Sheet-braided'	Succession consisting near-entirely of beds with aspect ratios exceeding 20:1 (McMahon and Davies, 2018b)
Fluvial style	A character of an alluvial rock sequence, opposed to an interpretation of fluvial processes
Architectural element	A package of strata formed by a distinct fluvial process (List of architectural elements in Table 3)
Architectural deposit	Genetically related package of strata which comprises multiple architectural elements (for example, a barform deposit may comprise of multiple downstream-accretion elements overlain by an upper-flow-regime element).
Sequence	Vertical succession of multiple architectural deposits.

1513

1514

1515

1516

1517

1518

1519

1520

1521

1522

1523

1524 Table 3

Element	Acronym	Description
Sandy bedforms	SB	Sand-grade elements not genetically related to their underlying surface.
Downstream-accretion element	DA	Bedform migration ±30° down-slope of a genetically related underlying surface
Downstream-lateral-accretion element	DLA	Bedform migration 30°-60° down-slope of a genetically related underlying surface
Lateral-accretion-element	LA	Bedform migration 60°-120° of the underlying surface
Upstream-accretion element	UA	Bedform migration ±30° up-slope of a genetically related underlying surface
Upstream-lateral-accretion element	ULA	Bedform migration 30°-60° up-slope of a genetically related underlying surface
Upper-flow-regime element	UFR	Any element comprising bedforms which developed under upper-flow regime conditions.
Floodplain fines	FF	Deposits of overbank sheetflow, floodplain ponds and swamps
Abandoned channel fills	FF(CH)	Like CH elements, FF(CH) elements have an underlying erosional concave-up geometry, but channel fill is typically mud-silt grade.

1525

1526

1527

1528

1529

1530

1531

1532

1533

1534 Table 4

Location	**Average thickness**	**Estimated position in vertical succession**
Stoer Peninsula and Suilven	2.60 (n = 7)	Lower third
Stac Pollaidh, Achiltibuie, Liathach, Alligin, Torridon	3.68 (n = 20)	Middle third
Applecross, Bealach na Bà	5.47 (n = 6)	Upper third

1535